NATIONAL ADVISORY COMMITTEE
FOR AERONAUTICS

TECHNICAL NOTE 2412

THEORETICAL FORCE AND MOMENTS DUE TO SIDESLIP

OF A NUMBER OF VERTICAL TAIL CONFIGURATIONS

AT SUPERSONIC SPEEDS

By John C. Martin and Frank S. Malvestuto, Jr.

Langley Aeronautical Laboratory
Langley Field, Va.

Washington

September 1951

1

NATIONAL ADVISORY COMMITTEE FOR AERONAUTICS

———

TECHNICAL NOTE 2412

———

THEORETICAL FORCE AND MOMENTS DUE TO SIDESLIP

OF A NUMBER OF VERTICAL TAIL CONFIGURATIONS

AT SUPERSONIC SPEEDS

By John C. Martin and Frank S. Malvestuto, Jr.

SUMMARY

Formulas have been obtained by means of the linearized supersonic-flow theory for the lateral force due to sideslip C_{Y_β}, the yawing moment due to sideslip C_{n_β}, and the rolling moment due to sideslip C_{l_β} for normal tail arrangements consisting of rectangular, triangular, and sweptback vertical tails of arbitrary taper and sweep mounted symmetrically on a horizontal tail of arbitrary shape. The results are restricted to cases where the leading edges are supersonic and the Mach line from the tip of the leading edge of the vertical tail does not intersect the root section.

The effect of the horizontal tail on the derivatives was evaluated for the cases where the Mach line from the leading edge of the root section cuts the trailing edge of the vertical tail.

A series of design curves is presented which permits rapid estimation of the lateral force due to sideslip C_{Y_β}, the yawing moment due to sideslip C_{n_β}, and the rolling moment due to sideslip C_{l_β}.

INTRODUCTION

With the advent of flight at supersonic speeds the dynamic stability of airplanes has become a serious consideration. The conceptions and usage of the linearized theory of supersonic flow enable an evaluation of a first-order approximation of the stability derivatives. Stability derivatives are now available for various wing plan forms at supersonic speeds. (See bibliography of reference 1 and references of reference 2.)

Information on the stability derivatives contributed by the vertical tail, which have an important effect on lateral stability, is lacking. A theoretical analysis is presented in this paper to determine the lateral force, the yawing moment, and the rolling moment due to sideslip for a series of tail configurations that consist of vertical tails mounted symmetrically on a horizontal tail. The tail configurations considered herein are characterized by supersonic leading edges. The vertical-tail plan form may be either triangular, rectangular, or swept-back with arbitrary taper and sweep; whereas the horizontal tail may be arbitrary except for the rolling-moment derivative for which case the trailing edge must be swept at a constant angle. Consideration is also given to the magnitude of the end-plate effect of the horizontal tail on the values of the stability derivatives. From a knowledge of the derivative for the vertical- and horizontal-tail combination and the end-plate effect on this derivative, the derivative of a vertical tail with horizontal tail removed was obtained. These results are the limits of the case where the horizontal tail has subsonic edges, and the value of the stability derivative when the edges of the horizontal tail are subsonic are expected, therefore, to lie between the values of the derivative with the horizontal tail (all edges supersonic) attached to the vertical tail and the values of the derivatives for the vertical tail alone.

The calculations of the loading distributions that lead to the sideslip derivatives for nonplanar bodies, such as a tail configuration, are somewhat complex in the large. For a range of Mach number for which the leading edges of the tail plan forms are supersonic the load distribution due to sideslip over the horizontal and vertical tail can, however, be determined rather simply. For a normal tail assemblage, this simplification of the analysis results from the fact that the flow fields within the Mach cone from the apex of the system are physically separated by the horizontal and vertical tail surfaces and, therefore, do not inter-act. The load distributions for such systems may be determined by an application of planar methods together with the evaluation of the induced load effects if any.

In order to facilitate the use of the formulas and charts presented herein for the estimation of the stability derivatives, a detailed method of procedure has been included in the paper.

SYMBOLS

A   aspect ratio of vertical tail

$A' = BA$

$$B = \sqrt{M^2 - 1}$$

b_v span of vertical tail

b_w span of wing

c_r root chord

C_p nondimensional pressure coefficient

c chord

$$J = A'(1 + \lambda)$$

$$K = \frac{\text{Slope of leading edge}}{\text{Slope of trailing edge}} = \frac{\cot \Lambda_{TE}}{\cot \Lambda} = \frac{A'(1 + \lambda) \cdot}{A'(1 + \lambda) - 2m'(1 - \lambda)}$$

l distance from z-axis to leading edge of arbitrary section
          of vertical tail

l_t distance from center of gravity to root section of vertical .
          tail

L_y spanwise loading

M free-stream Mach number

m slope of leading edge of vertical tail

m_o slope of trailing edge of horizontal tail

$m' = Bm$

ΔP pressure difference across lifting surface

$$q = \frac{1}{2} \rho V^2$$

S_v area of vertical tail

S_w area of wing

u, v, w x-, y-, and z-components of perturbation velocity, respectively

V free-stream velocity

x, y, z rectangular coordinates (see fig. 2)

x_a, z_a rectangular coordinates (see tables I and II)

$\overline{X}$ distance along x-axis to center of pressure of vertical tail
        in presence of horizontal tail (see fig. 2)

$\overline{Z}$ distance along z-axis to center of pressure of vertical tail
        in presence of horizontal tail (see fig. 2)

$\Delta\overline{X}$ increment in $\overline{X}$ due to removal of horizontal tail

$\Delta\overline{Z}$ increment in $\overline{Z}$ due to removal of horizontal tail

α angle of attack, radians

β sideslip angle, radians

λ taper ratio of vertical tail

Λ sweep angle of leading edge of vertical tail

Λ_{TE} sweep angle of trailing edge of vertical tail

ρ free-stream density

ϕ perturbation surface velocity potential

C_Y lateral-force coefficient $\left(\dfrac{\text{Lateral force}}{\frac{1}{2}\rho V^2 S_v}\right)$

C_n yawing-moment coefficient $\left(\dfrac{\text{Yawing moment}}{\frac{1}{2}\rho V^2 b_v S_v}\right)$

C_l rolling-moment coefficient $\left(\dfrac{\text{Rolling moment}}{\frac{1}{2}\rho V^2 b_v S_v}\right)$

$$C_{Y_\beta} = \frac{\partial C_Y}{\partial \beta}$$

$$C_{n_\beta} = \frac{\partial C_n}{\partial \beta}$$

$$C_{l_\beta} = \frac{\partial C_l}{\partial \beta}$$

C_L wing lift coefficient

$$C_{L_\alpha} = \left(\frac{\partial C_L}{\partial \alpha}\right)_{\alpha \to 0}$$

$\left(C_Y\right)_t$ lateral-force coefficient of vertical and horizontal tail

$\left(C_n\right)_t$ yawing-moment coefficient of vertical and horizontal tail

$\left(C_l\right)_t$ rolling-moment coefficient of vertical and horizontal tail

$\left(C_Y\right)_v$ lateral-force coefficient of vertical tail without horizontal tail attached

$\left(C_n\right)_v$ yawing-moment coefficient of vertical tail without horizontal tail attached

$\left(C_l\right)_v$ rolling-moment coefficient of vertical tail without horizontal tail attached

$$\left(C_{Y_\beta}\right)_t = \left[\frac{\partial \left(C_Y\right)_t}{\partial \beta}\right]_{\beta \to 0}$$

$$\left(C_{n_\beta}\right)_t = \left[\frac{\partial \left(C_n\right)_t}{\partial \beta}\right]_{\beta \to 0}$$

$$\left(C_{l_\beta}\right)_t = \left[\frac{\partial \left(C_l\right)_t}{\partial \beta}\right]_{\beta \to 0}$$

$$\left(C_{Y_\beta}\right)_v = \left[\frac{\partial \left(C_Y\right)_v}{\partial \beta}\right]_{\beta \to 0}$$

$$\left(C_{n_\beta}\right)_v = \left[\frac{\partial \left(C_n\right)_v}{\partial \beta}\right]_{\beta \to 0}$$

$$\left(C_{l_\beta}\right)_v = \left[\frac{\partial \left(C_l\right)_v}{\partial \beta}\right]_{\beta \to 0}$$

C_{Y_β}', C_{n_β}', C_{l_β}' contribution of tail to sideslip derivatives about
             stability axes based on wing area and span; values
             apply to vertical- and horizontal-tail combinations
             unless otherwise noted

$\left(C_{l_\beta}\right)_{vt}$ contribution to $\left(C_{l_\beta}\right)_t$ of pressure difference across
             vertical tail in presence of horizontal tail

$\left(C_{l_\beta}\right)_{ht}$ contribution to $\left(C_{l_\beta}\right)_t$ of pressure difference across
             horizontal tail in presence of vertical tail

$\Delta\left(C_{Y_\beta}\right)_t$ change in $\left(C_{Y_\beta}\right)_t$ due to horizontal tail

$\Delta\left(C_{n_\beta}\right)_t$ change in $\left(C_{n_\beta}\right)_t$ due to horizontal tail

$\Delta\left(C_{l_\beta}\right)_{vt}$ change in $\left(C_{l_\beta}\right)_{vt}$ due to horizontal tail

ANALYSIS

Scope

The tail configurations considered in this paper are sketched in figure 1. The orientation of the tail with respect to a body system of coordinate axes used in the analysis is shown in figure 2(a). Figure 2(b) shows a typical tail oriented with respect to the stability-axes system. The stability derivatives are generally evaluated in this system for stability studies.

The analysis is limited to tail configurations having surfaces of vanishingly small thickness and of zero camber. The vertical tail is assumed to be yawed an infinitesimal amount $(\beta \rightarrow 0)$; whereas the horizontal tail is always at zero geometric angle of attack. Essentially then, the vertical tail produces the disturbance velocities (similar to a wing at an angle of attack) and the horizontal tail acts as a barrier or end plate to the propagation of the vertical-tail disturbances (similar to end plate attached to lifting wing).

For the tail arrangements considered in this paper, the horizontal tail must completely shield the root chord of the vertical tail; thus, the leading edge of the root chord of the horizontal tail must at least coincide with or be forward of the leading edge of the root chord of the vertical tail and, similarly, the trailing edge of the root chord of the

horizontal tail must coincide with or be in back of the trailing edge of the root chord of the vertical tail. The results to be presented in the following sections for the vertical tail completely shielded by the horizontal tail and for the vertical-tail-alone case may be used, however, to obtain rough estimations of the derivatives for tail arrangements for which the horizontal tail does not completely shield the root chord of the vertical tail. Estimates can be made in this manner by interpolation with a fair degree of accuracy because the end-plate effect of the horizontal tail is relatively small even for the cases considered in this paper where the horizontal tail is a perfect end plate.

The stability derivatives are valid for a range of Mach number for which the leading and trailing edges of the tail surfaces are supersonic; that is, the Mach number of the flow component normal to these edges is greater than 1. The results for the derivatives $\left(C_{Y_\beta}\right)_t$ for the case of vertical-tail - horizontal-tail combinations have the added restriction that the Mach line from the tip of the leading edge of the vertical tail does not intersect the root section. The derivatives $\left(C_{n_\beta}\right)_t$ and $\left(C_{l_\beta}\right)_t$ have the same restriction as mentioned previously and a further restriction which requires that the Mach line from the root section must intersect the trailing edge of the vertical tail. For the derivatives $\left(C_{n_\beta}\right)_t$ and and $\left(C_{l_\beta}\right)_t$, however, values were obtained for the limiting case for which the Mach line from the root section is coincident with the leading edge of the vertical tail. From this result, together with the results obtained when the Mach line intersects the trailing edge, an estimation of the values of the derivatives $\left(C_{n_\beta}\right)_t$ and $\left(C_{l_\beta}\right)_t$ can be obtained for the range of Mach number where the Mach line from the root section cuts the tip of the vertical tail. The results for the effect of the horizontal tail (the so-called end-plate effect) on the derivatives are restricted to cases where the Mach line from the root section cuts the trailing edge of the vertical tail and to cases where the Mach line from the leading edge of the tip of the vertical tail does not intersect the root section.

Basic Considerations

The evaluation of the tail contribution to the derivatives C_{Y_β}, C_{n_β}, and C_{l_β} essentially involves a knowledge of the lifting-pressure distribution over the tail surfaces associated with sideslip (angle of attack of the vertical tail). The lifting-pressure coefficient can be determined from the perturbation velocity potential by the well-known

relationship

$$\Delta C_p = \frac{\Delta P}{\frac{1}{2}\rho V^2} = \frac{2}{V}\Delta u$$

or

$$\Delta C_p = \frac{2}{V}\frac{\partial}{\partial x}\Delta\phi(x,y,z) \tag{1}$$

where $\Delta\phi$ is the velocity-potential difference across the surface. Equation (1) is consistent with the small perturbation theory only if the magnitudes of the perturbation velocities are equal across the lifting surface. When the magnitudes of the perturbation velocities are not equal across the lifting surface, equation (1) should contain differences in the squares of the velocities v and w. The squared terms lead to derivatives which are linear functions of θ; therefore, these terms will vanish because the derivatives are to be evaluated as $\beta\rightarrow 0$.

The real problem of finding the pressure distribution over the tail surfaces is therefore to find the velocity potential on each side of each tail surface. The tail configurations considered, as mentioned previously, are of the nonplanar type and are, of course, unsymmetrical with respect to the y- and z-axes. The determination of the velocity potential or its derivatives for nonplanar systems of the unsymmetrical type is usually quite difficult, particularly when the leading and trailing edges of the configuration are subsonic. For these same tail configurations, however, when the leading and trailing edges of the horizontal tail are supersonic, linearized expressions for the surface velocity potential and lifting pressures may be easily obtained. If reference is made to the sketches of the tail configurations presented in figure 1, it can be seen that so long as the leading and trailing edges of the horizontal tail surfaces are supersonic, the horizontal tail acts as a reflecting plane. The flow over the lower surface of the horizontal tail is therefore undisturbed; hence, the component of perturbation velocity in the plane of the horizontal tail surface is zero. The solution for the potential in the region affected by the vertical tail is therefore the solution for a symmetrical lifting surface which is made up of the vertical tail surface and its reflection through the horizontal tail surface. The potential remains unchanged if the horizontal tail is altered outside the Mach sheet from the leading edge of the vertical tail.

As stated previously, only the potential on each side of each surface is needed. The potential and pressure across the vertical tail surfaces considered herein can be determined directly from the results given in reference 3. Formulas for these potentials and pressures are presented for convenience in tables I and II, respectively. It should be noted that the potential and the perturbation pressure are zero on the lower

surface of the horizontal tail. The potential and perturbation pressure
on the upper surface of the horizontal tail were found from the potential
solution for a lifting surface made up of the vertical tail surface and
its reflection in the horizontal tail. The source-distribution method
presented in reference 4 was used to find these potentials and the corre-
sponding pressures. The expressions for the potentials and pressures on
the horizontal tail surface are presented in tables I and II, respectively.

If the horizontal tail has subsonic edges in the region behind the
Mach sheet from the leading edge of the vertical tail, the potentials
and pressures for the horizontal tail given in tables I and II are no
longer correct. Similarly, if the horizontal tail has a subsonic leading
or trailing edge in the region behind the Mach sheet from the leading
edge of the vertical tail and if the subsonic-edge disturbances affect
the vertical tail, then the pressure and potential given in tables I
and II for the vertical tail are also invalid.

A rough qualitative estimation of the effect of the subsonic edges
of the horizontal tail on the derivatives considered herein was obtained
by the evaluation of the so-called end-plate effect of the horizontal
tail, that is, the change in the values of the derivatives for the complete
configuration when the horizontal tail with all edges supersonic is
completely removed from the vertical tail. The values of the stability
derivatives when the edges of the horizontal tail are subsonic are expected
to be somewhere between the value of the derivatives with the horizontal
tail (all edges supersonic) attached to the vertical tail and the values
of the derivatives for the vertical tail alone. The expressions for the
potentials and pressures for the vertical tail alone were obtained by an
application of Evvard's method (reference 5) and are presented in tables I
and II. Illustrative plots of the chordwise and spanwise pressure distri-
butions across the vertical tail with and without the horizontal tail are
given in figure 3. Figure 4 shows illustrative plots of the chordwise
and spanwise pressure distributions of the induced pressure on the hori-
zontal tail. Illustrative plots of the spanwise loadings for the vertical
and horizontal tails are presented in figure 5.

$$\text{Derivative } \left(C_{Y_\beta}\right)_t$$

The nondimensional lateral force due to sideslip derivative may be
expressed as

$$\left(C_{Y_\beta}\right)_t = \frac{\text{Lateral force}}{\beta q S_v}$$

The lateral force can be obtained by integrating the pressure distribution
over the vertical tail surface in sideslip. (See table I.) The pressure
distribution over the vertical tail in the presence of the horizontal tail

is the same as that for a wing which is composed of the area of the vertical tail and its reflection in the horizontal tail. The magnitude of the derivative $\left(C_{Y_\beta}\right)_t$ of the vertical tail, therefore, is the lift-curve slope C_{L_α} of a wing of which the vertical tail is one panel (semispan of wing). Formulas for $\left(C_{Y_\beta}\right)_t$ were obtained by transforming the results for C_{L_α} presented in reference 3. Since the vertical tail is a duplicate of one panel of the wing, the transformation merely consists in replacing the aspect ratio of the wing by twice the aspect ratio of the vertical tail. The resulting expressions for $\left(C_{Y_\beta}\right)_t$ in terms of the aspect ratio of the vertical tail are as follows:

Mach line from the root section coincident with leading edge:

For an arbitrary taper ratio,

$$\left(C_{Y_\beta}\right)_t = \frac{-4A'}{\pi B}\left\{ \frac{K\sqrt{K-1}}{(1-\lambda)^2(K+1)\sqrt{K+1}}\left[\cos^{-1}(2\lambda-1) - \cos^{-1}\frac{1}{K}\right] - \right.$$

$$\frac{\lambda\sqrt{\lambda(K-1)}}{(1-\lambda)\sqrt{(1-\lambda)(K+1)}} + \frac{K-1}{K(1-\lambda)^2(K+1)} +$$

$$\left. \frac{\left[2K-\lambda(K+1)\right]^2}{2\sqrt{2}(1-\lambda)^2(K+1)\sqrt{K}\sqrt{K+1}}\cos^{-1}\frac{2K+\lambda(1-3K)}{2K-\lambda(K+1)} \right\} \qquad (2)$$

For a taper ratio of 1,

$$\left(C_{Y_\beta}\right)_t = \frac{-1}{\pi A'B}\left[\frac{(1+2A')^2}{2}\cos^{-1}\frac{2A'-1}{2A'+1} + \right.$$

$$\left. \sqrt{2A'} - \frac{8}{3} + \frac{10A'}{3}\sqrt{2A'} \right] \qquad (3)$$

Mach line from the root section cuts the tip:

For an arbitrary taper ratio,

$$\left(C_{Y_\beta}\right)_t = \frac{-1}{\pi B \sqrt{m'^2 - 1}} \left(\frac{2\left[2m'K + A'(K - 1)\right]^2}{A'(K^2 - 1)} \left\{ \frac{1}{K} \cos^{-1} \frac{1}{m'} + \right. \right.$$

$$\left. \frac{K\sqrt{m'^2 - 1}}{\sqrt{Km' + 1}\sqrt{Km' - 1}} \left[\cos^{-1} \frac{-1}{Km'} - \cos^{-1} \frac{2Km'(2A' - 1) - A'(K + 3)}{2Km' + A'(K - 1)} \right] \right\} -$$

$$\frac{\left[2m'K - A'(K - 1)\right]^2 \sqrt{m' + 1}}{A'(K - 1)\sqrt{K}\sqrt{Km' + 1}} \cos^{-1} \frac{2Km'(1 - 2A') + A'(3K + 1)}{2Km' - A'(K - 1)} +$$

$$\left. \frac{\left[2m'K + A'(1 + 3K)\right]^2 \sqrt{m' - 1}}{A'(K + 1)\sqrt{K}\sqrt{Km' + 1}} \cos^{-1} \frac{2Km'(2A' - 1) + A'(K - 1)}{2Km' + A'(3K + 1)} \right) \qquad (4)$$

For a taper ratio of 1,

$$\left(C_{Y_\beta}\right)_t = \frac{-2}{\pi A'B\sqrt{m'^2 - 1}} \left\{ -\frac{m'^2(m'^2 - 2)}{m'^2 - 1} \cos^{-1}\frac{1}{m'} - \frac{m'^2}{\sqrt{m'^2 - 1}} + \right.$$

$$\left[\frac{m'^2(m' - 2)}{2(m' - 1)} + 2A'm'\right] \cos^{-1}\frac{m' - 2A'(m' - 1)}{m'} +$$

$$\frac{(m' + 2A')^2\sqrt{m' - 1}}{2\sqrt{m' + 1}} \cos^{-1}\frac{m'(2A' - 1)}{2A' + m'} +$$

$$\left. \frac{m'\sqrt{A'[m' - A'(m' - 1)]}}{\sqrt{m' - 1}} \right\} \tag{5}$$

Mach line from the root section cuts the trailing edge:

For an arbitrary taper ratio,

$$\left(C_{Y_\beta}\right)_t = \frac{-1}{B\pi\sqrt{m'^2 - 1}} \left\{ \frac{2[2m'K + A'(K - 1)]^2}{A'(K^2 - 1)} \left(\frac{1}{K}\cos^{-1}\frac{1}{m'} + \right. \right.$$

$$\left. \frac{K\sqrt{m'^2 - 1}}{\sqrt{Km' - 1}\sqrt{Km' + 1}} \cos^{-1}\frac{-1}{Km'}\right) \frac{-\pi[2Km' - A'(K - 1)]^2\sqrt{m' + 1}}{A'(K - 1)\sqrt{K}\sqrt{Km' + 1}} \tag{6}$$

For a taper ratio of 1,

$$\left(C_{Y_\beta}\right)_t = \frac{-2}{\pi B A' \sqrt{m'^2 - 1}} \left\{ -\frac{m'^2(m'^2 - 2)}{m'^2 - 1} \cos^{-1}\frac{1}{m'} - \frac{m'^2}{\sqrt{m'^2 - 1}} + \left[\frac{m'^2(m' - 2)}{2(m' - 1)} + 2A'm'\right] \pi \right\} \tag{7}$$

For an arbitrary taper ratio where $K = \infty$ or 0,

$$\left(C_{Y_\beta}\right)_t = \frac{-4A'}{B(1 - \lambda)} \left\{ \frac{1}{J} - \frac{\lambda^2}{\sqrt{J[J - 2(1 - \lambda)]}} \right\} \tag{8}$$

For rectangular vertical tails,

$$\left(C_{Y_\beta}\right)_t = \frac{-4}{B}\left(1 - \frac{1}{4A'}\right) \tag{9}$$

The effect of the horizontal tail on the derivative $\left(C_{Y_\beta}\right)_t$ was evaluated by integrating the pressure distribution over the vertical tail that is induced by the horizontal tail. The induced pressure distribution was obtained by subtracting the pressure distribution of an isolated panel at an angle of attack (or sideslip) from the pressure distribution of the vertical tail with horizontal tail attached. The corresponding nondimensional increment to the lateral-force derivative is given by the following equations:

Mach line from the root section cuts the trailing edge:

For an arbitrary taper ratio,

$$\Delta\left(C_{Y_\beta}\right)'_t = \frac{16m'}{B\pi J(1 + \lambda)}\left[\frac{-K}{(1 - K^2)\sqrt{m'^2 - 1}}\cos^{-1}\frac{1}{m'} + \right.$$

$$\left.\frac{K^2\pi}{2(1 - K)\sqrt{K}\sqrt{(m'K - 1)(m' + 1)}} - \frac{K^3}{(1 - K^2)\sqrt{Km' + 1}\sqrt{Km' - 1}}\cos^{-1}\frac{-1}{Km'}\right] \qquad (10)$$

For a taper ratio of 1,

$$\Delta\left(C_{Y_\beta}\right)_t = \frac{4m'^2}{\pi BA'}\left[\frac{2 - m'^2}{2(m'^2 - 1)^{3/2}}\cos^{-1}\frac{1}{m'} - \frac{1}{2(m'^2 - 1)} + \frac{\pi(m' + 2)}{4(m' + 1)\sqrt{m'^2 - 1}}\right] \qquad (11)$$

For an arbitrary taper ratio where the leading or trailing edge is perpendicular to the free-stream direction,

$$\Delta\left(C_{Y_\beta}\right)_t = \frac{4}{B(1 - \lambda)}\left\{\frac{-\sqrt{A'}}{\sqrt{(1 + \lambda)\left[A'(1 + \lambda) + 2(1 - \lambda)\right]}} + \frac{1}{1 + \lambda}\right\} \qquad (12)$$

For rectangular vertical tails,

$$\Delta\left(C_{Y_\beta}\right)_t = \frac{1}{A'B} \tag{13}$$

Data taken from reference 2 were used to obtain curves for $B\left(C_{Y_\beta}\right)_t$ for taper ratios of 0, 1/2, and 1 for various values of sweep angle, Mach number, and aspect ratio. These data are presented in figure 6. Calculations for the effect of the horizontal tail on the derivative $\left(C_{Y_\beta}\right)_t$ were made. These calculations are presented in figure 7 for taper ratios of 0, 1/2, and 1 for various values of sweepback angle, Mach number, and aspect ratio.

Figure 8 presents some illustrative variations of the derivative C_{Y_β}' with and without the horizontal tail for various values of Mach number, aspect ratio, sweep angle, and taper ratio.

Since the derivative $\left(C_{Y_\beta}\right)_t$ and the effect of the horizontal tail on this derivative are based on the area of the vertical tail, both $\left(C_{Y_\beta}\right)_t$ and $\Delta\left(C_{Y_\beta}\right)_t$ must be multiplied by the ratio S_V/S_W before they are used in stability calculations. Since the lateral force is the same for both body and stability axes, then C_{Y_β}' and $\left(C_{Y_\beta}\right)_t$ are related by the equation $C_{Y_\beta}' = \frac{S_V}{S_W}\left(C_{Y_\beta}\right)_t$.

Derivative $\left(C_{n_\beta}\right)_t$

It is convenient to express the yawing moment due to sideslip of the vertical tail relative to the body axes, the origin of which is located at the center of gravity of the airplane a distance l_t from the leading edge of the root section of the vertical tail. The yawing moment of the vertical tail in the presence of the horizontal tail is then given non-dimensionally as

$$\left(C_{n_\beta}\right)_t = \left(C_{Y_\beta}\right)_t\left(\frac{\overline{X}}{b_V} + \frac{l_t}{b_V}\right) \tag{14}$$

where $\bar{X}$ is the x-component of the distance of the center of pressure of the vertical tail from the leading edge of the root section, and l_t is the distance along the x-axis between the center of gravity of the airplane and the leading edge of the root section of the vertical tail.

The distance $\bar{X}$ was calculated in the usual manner from a consideration of the moment due to pressure distribution over the vertical tail surface. The resulting equations for the distances $\bar{X}$ are as follows:

Mach line from the root section coincident with the leading edge:

For an arbitrary taper ratio,

$$\bar{X} = \frac{2b_v\left[J^3(K-1)^2 - 6J^2K(K-1) + 12JK^2\right]}{\left(C_{Y_\beta}\right)_t 3\pi K^2(1+\lambda)(\lambda^2+\lambda+1)}\left[\left\{\frac{4K(1-4K^2)}{J^3(1-K^2)^2} + \right.\right.$$

$$\frac{\left[J^2(K-1)^2(2K^2+6K+7) - 4JK(K-1)(4K^2-3K-16) + 12K^2(18K^2-K-2)\right]\sqrt{2K+J(1-K)}}{15J^2(1-K^2)^2\sqrt{J(1+K)}} -$$

$$\frac{4K^3(1+2K^2)}{J^3(1-K^2)^2\sqrt{K+1}\sqrt{K-1}}\left(\cos^{-1}\frac{J(1-K)+K}{K} - \cos^{-1}\frac{1}{K}\right)\right\} -$$

$$2\sqrt{2}\left(\frac{(4JK+J-18K)\sqrt{(4K-2JK+2J)^3}}{30\left[J(K+1)\right]^{5/2}} - \frac{2K^2(4-J)-(JK-J-2K)}{JK(1+K)}\left\{\frac{-(J+2K-3KJ)\sqrt{2K-JK+J}}{2\left[2J(K+1)\right]^{3/2}} - \right.\right.$$

$$\left.\left.\left.\frac{(JK+J+2K)^2K^{1/2}}{8J(1+K)^{3/2}}\cos^{-1}\frac{3JK-J-2K}{JK+J+2K}\right\}\right)\right] \tag{15}$$

For a taper ratio of 1,

$$\overline{X} = \frac{1}{\left(C_{Y_\beta}\right)_t}\left(\frac{-2b_v}{45\pi A'\sqrt{2A'}}\left[4(36A'^2 + 20A' + 9) - \frac{56}{\sqrt{2A'}}\right] + \right.$$

$$\frac{4b_v\sqrt{2}}{3\pi\sqrt{A'}}\left\{\frac{9 - 5A'}{15A'} - \frac{2A' - 5}{16A'}\left[(2A' - 1) - \right.\right.$$

$$\left.\left.\left.\frac{(2A' + 1)^2}{2\sqrt{2A'}}\cos^{-1}\frac{2A' - 1}{2A' + 1}\right]\right\}\right) \tag{16}$$

Mach line from the root section cuts the trailing edge:

For an arbitrary taper ratio,

$$\overline{X} = \frac{-32m'b_v}{\pi\left(C_{Y_\beta}\right)_t J^2(1 + \lambda)\sqrt{m'^2 - 1}}\left\{\frac{Km'(3K^2 - 1)}{3(K^2 - 1)^2}\cos^{-1}\frac{1}{m'} + \frac{K^3m'\sqrt{m'^2 - 1}}{2(K^2 - 1)(K^2m'^2 - 1)} + \right.$$

$$\frac{K^3m'(2m'^2K^4 - K^2 - 1)\sqrt{m'^2 - 1}}{3(K^2 - 1)^2(m'^2K^2 - 1)\sqrt{m'K + 1}\sqrt{m'K - 1}}\cos^{-1}\frac{-1}{Km'} +$$

$$\frac{[2m'K - J(K - 1)]^2\pi}{8}\left[\frac{(1 - 4m'K^2 + 2m'K - 3K)\sqrt{m' + 1}}{6m'(K - 1)^2(1 + m'K)\sqrt{K}\sqrt{1 + m'K}} - \right.$$

$$\left.\left.\frac{J(3K + 2m'K^2 + 2m'K + 1)\sqrt{m' + 1}}{12Km'^2(K - 1)(1 + m'K)\sqrt{K}\sqrt{1 + m'K}}\right]\right\} \tag{17}$$

For a taper ratio of 1,

$$
\overline{X} = \frac{-b_v}{\left(C_{Y_\beta}\right)_t A'^2} \left[\frac{m'^2(-3m'^4 + 10m' - 4)}{3\pi(m'^2 - 1)^2 \sqrt{m'^2 - 1}} \cos^{-1} \frac{1}{m'} - \frac{m'^4}{\pi(m'^2 - 1)^2} + \frac{2A'^2}{\sqrt{m'^2 - 1}} + \frac{A'(2m'^2 + m')}{(m' + 1)\sqrt{m'^2 - 1}} + \frac{6m'^6 - 8m'^5 - 17m'^4 + 2m'^3 + 5m'^2}{12(m'^2 - 1)^2\sqrt{m'^2 - 1}} \right] \qquad (18)
$$

An expression for $\overline{X}$ in a somewhat different form from the preceding equations is presented in reference 6. The values of $\left(C_{Y_\beta}\right)_t$ used in the preceding equations must of course be valid for the particular Mach line arrangement over the tail for which the distance $\overline{X}$ is to be determined.

The results for the derivative $\left(C_{n_\beta}\right)_t$ are given relative to a system of body axes located at the leading edge of the root section. (See fig. 2.) The transformation formulas for conversion from body axes to stability axes are given in reference 7. To the first order in α (small angles of attack) the formula for the contribution of the tail to the derivative C_{n_β}', based on the wing area and wing span, is given by

$$
C_{n_\beta}' = \frac{b_v S_v}{b_w S_w} \left[\left(C_{n_\beta}\right)_t - \alpha\left(C_{l_\beta}\right)_t \right] \qquad (19)
$$

where the prime refers to the stability axes with the origin located at the center of gravity of the airplane.

The end-plate effect of the horizontal tail on the derivative $\left(C_{n_\beta}\right)_t$ may be expressed in terms of the change in the center-of-pressure distance $\overline{X}$ and the change in $\left(C_{Y_\beta}\right)_t$. The change $\Delta\overline{X}$ in the center-of-pressure distance $\overline{X}$ is equal to the difference in the distance $\overline{X}$ with the horizontal tail attached to the vertical tail and with the vertical tail alone. Mathematically, the increment in $\overline{X}$ is given by

$$
\Delta\overline{X} = \frac{\overline{X}\left(C_{Y_\beta}\right)_t + b_v \Delta\left(C_{n_\beta}\right)_t}{\left(C_{Y_\beta}\right)_t + \Delta\left(C_{Y_\beta}\right)_t} - \overline{X} \qquad (20)
$$

where the quantities $\overline{X}$, $\left(C_{Y_\beta}\right)_t$, and the change in $\left(C_{Y_\beta}\right)_t$ due to the horizontal tail, have previously been determined. The quantity $\Delta\left(C_{n_\beta}\right)_t$ depends upon the plan-form geometry and Mach line location. For the condition where the Mach line from the leading edge of the root section cuts the trailing edge, $\Delta\left(C_{n_\beta}\right)_t$ is given by the following expressions:

For an arbitrary taper ratio,

$$\Delta\left(C_{n_\beta}\right)_t = \frac{32m'^2K^3}{3\pi A'^2(1+\lambda)3\sqrt{m'^2-1}}\left[\frac{3K^2-1}{K^2(1-K^2)^2}\cos^{-1}\frac{1}{m'} - \frac{\sqrt{m'^2-1}}{(m'^2K^2-1)(1-K^2)} + \right.$$

$$\left. \frac{(2m'^2K^4-K^2-1)\sqrt{m'^2-1}}{(1-K^2)^2(m'^2K^2-1)\sqrt{m'K+1}\sqrt{m'K-1}}\cos^{-1}\frac{-1}{Km'} + \frac{\sqrt{m'-1}(3K+2Km'-4K^2m'-1)\pi}{4K(1-K)^2(m'K-1)\sqrt{K}\sqrt{m'K-1}}\right] \quad (21)$$

For a taper ratio of 1,

$$\Delta\left(C_{n_\beta}\right)_t = \frac{4m'^2}{3A'^2\pi\sqrt{m'^2-1}}\left[-\frac{3m'^4-10m'^2+4}{4(m'^2-1)^2}\cos^{-1}\frac{1}{m'} - \frac{3m'^2}{4(m'^2-1)^{3/2}} + \frac{\pi(6m'^3+14m'^2-3m'-5)}{16(m'^2-1)(m'+1)}\right]$$

$$(22)$$

For a straight trailing edge,

$$\Delta\left(C_{n_\beta}\right)_t = \frac{16}{3(1-\lambda)}\left\{\frac{1}{A'(1+\lambda)^2} - \frac{1}{(1+\lambda)\sqrt{A'(1+\lambda)}\left[A'(1+\lambda)+2(1-\lambda)\right]}\right\} \quad (23)$$

For a leading edge which is perpendicular to the free-stream direction,

$$\Delta\left(C_{n_\beta}\right)_t = \frac{8}{3}\left(\frac{1}{1-\lambda}\left\{\frac{1}{A'(1+\lambda)} - \right.\right.$$

$$\left.\left.\frac{(1-\lambda)+A'(1+\lambda)}{\left[2(1-\lambda)+A'(1+\lambda)\right]\sqrt{A'(1+\lambda)\left[2(1-\lambda)+A'(1+\lambda)\right]}}\right\}\right) \quad (24)$$

For rectangular vertical tails,

$$\Delta\left(C_{n_\beta}\right)_t = \frac{2}{3(A')^2} \qquad (25)$$

As previously indicated, the derivative $\left(C_{n_\beta}\right)_t$ may be expressed in terms of the derivative $\left(C_{Y_\beta}\right)_t$ and an arm $\overline{X}$. Calculations for the distance $\overline{X}$ were made for taper ratios of 0 and 1 for various values of sweep angle, aspect ratio, and Mach number. These results are presented in figure 9. Since the formulas for $\overline{X}$ for the case where the Mach line from the root section of the vertical tail cuts the tip were not found, the curves for $\overline{X}$ were faired through this region. The faired parts of the curves are dashed in figure 9. The change in the distance $\overline{X}$ due to the horizontal tail was calculated for taper ratios of 0 and 1. The results of these calculations are given in figure 10. Figure 11 presents some illustrative variations of the derivative C_{n_β}' with and without the horizontal tail for various values of Mach number, aspect ratio, and sweep angle.

Derivative $\left(C_{l_\beta}\right)_t$

The rolling moment due to sideslip may be calculated by integrating the moment of the pressure loading about the root chord of the vertical tail. Although the pressure distribution over the horizontal tail does not contribute to the lateral force or yawing moment it does affect the rolling moment due to sideslip. The integrations of the first moments of the pressure for sideslip were therefore performed over both the vertical and horizontal tail surfaces.

The total rolling-moment derivative may be written as

$$\left(C_{l_\beta}\right)_t = \left(C_{l_\beta}\right)_{vt} + \left(C_{l_\beta}\right)_{ht} = \left(\frac{(\text{Lateral force})\bar{Z}}{qS_v b_v}\right) + \left(C_{l_\beta}\right)_{ht}$$

$$= \left(C_{Y_\beta}\right)_t \left(\frac{\bar{Z}}{b_v}\right) + \left(C_{l_\beta}\right)_{ht} \tag{26}$$

The first term of the preceding expression, which gives the vertical-tail contribution to the rolling moment, has been expressed in terms of a force $\left(C_{Y_\beta}\right)_t$ and an arm $\bar{Z}$. The rolling-moment arm $\bar{Z}$ was determined by evaluating the rolling moment (due to sideslip) about the x body axis and dividing the moment by the lateral force. For the condition where the Mach lines from the leading edge of the root chord are coincident with the leading edges, $\bar{Z}$ is given by the following expressions:

For a taper ratio of 1,

$$\bar{Z} = \frac{-8b_v}{A'^2 \pi B C_{Y_\beta}} \left\{ \frac{(2A' - 1)(2A' + 1)^2}{64} \cos^{-1} \frac{2A' - 1}{2A' + 1} + \frac{1}{15} + \right.$$

$$\left. \frac{\left[132A'^2 - 20A' - 15\right]\sqrt{2A'}}{480} \right\} \tag{27}$$

For an arbitrary taper ratio,

$$\bar{Z} = \frac{-64b_v}{J^2(1+\lambda)K\pi B C_{Y_\beta}} \left\{ \frac{K^3(2K^2+1)}{6(1-K^2)^2} - \frac{K^5}{2(1-K^2)^2\sqrt{K+1}\sqrt{K-1}} \left[\cos^{-1}\frac{1}{K} - \right. \right.$$

$$\left. \cos^{-1}\frac{J(1-K)+K}{K} \right] + \frac{\sqrt{2K}\left[J(1+K)-2K\right]\left[J(1+K)+2K\right]^2}{128(1+K)^2\sqrt{1+K}} \cos^{-1}\frac{J(3K-1)-2K}{J(1+K)+2K} +$$

$$\frac{K\left[J^2(1-K)^2(1+K)(7K+3)+8JK^2(1-K^2)-12K^2(1+K)^2\right]}{96(1-K^2)^2} \sqrt{\frac{J\left[J(1-K)+2K\right]}{1+K}} \right\} \tag{28}$$

For the configuration where the Mach line from the leading edge of the root chord cuts the trailing edge of the vertical tail, $\overline{Z}$ is given as follows:

For an arbitrary taper ratio,

$$\overline{Z} = \frac{-16b_v}{3J^2(1 + \lambda)B\left(C_{Y_\beta}\right)_t} \left\{ \frac{2K^2m'^3(1 + K^2)}{\pi(1 - K^2)^2\sqrt{m'^2 - 1}} \cos^{-1}\frac{1}{m'} + \right.$$

$$\frac{2K^4m'^3(-3 + 2K^2m'^2 + K^2)}{\pi\sqrt{Km + 1}\sqrt{Km - 1}(K^2m'^2 - 1)(1 - K^2)^2} \cos^{-1}\frac{-1}{Km'} - \frac{2K^4m'^3}{\pi(1 - K^2)(K^2m'^2 - 1)} +$$

$$\frac{J(1 - K) + 2m'K}{\sqrt{K}\sqrt{(1 + m'K)(m' - 1)}}\left[J^2(1 - K)^2\left(3K - K^2 + 3K^3 + 2K^2m' + 8K^3m' + \right.\right.$$

$$8m'^2K^3 + 6m'K + 3\right) + 4K^2m'J(1 - K)(m' + 1)(2m'K^2 + 3K^2 - 4K + 3) +$$

$$\left.\left. 4K^2m'^2(3K - 7K^2 - 10m'K^2 + 3K^3 + 2m'K^3 - 4m'^2K^3 - 3)\right] \frac{1}{32K(1 - K)^2(1 + m'K)^2} \right\} \quad (29)$$

For a taper ratio of 1,

$$\overline{Z} = \frac{-b_v}{A'^2B\left(C_{Y_\beta}\right)_t} \left\{ \frac{m'^3(4 - 2m'^2 + m'^4)}{3\pi(m'^2 - 1)^{5/2}} \cos^{-1}\frac{1}{m'} + \frac{m'^3(m'^2 - 4)}{3\pi(m'^2 - 1)^2} + \right.$$

$$\left. \frac{m'\left[24A'^2(m'^2 - 1)^2 - 12A'm'(m' + 1)(m' - 1)^2 + m'^2(-2m'^4 + 7m'^2 - 6m' - 11)\right]}{12(m'^2 - 1)^{5/2}} \right\} \quad (30)$$

An expression for $\bar{Z}$ in a different form for the cases given by equations (29) and (30) is presented in reference 6. The consideration regarding the contribution of the horizontal tail to the rolling moment due to sideslip $\left(C_{l_\beta}\right)_{ht}$ requires special emphasis. Because of its end-plate effect, the horizontal tail induces a pressure on the vertical tail. The vertical tail in turn induces on the horizontal tail a pressure field that is bounded by the trace on the horizontal tail of the Mach cone springing from the leading edge of the root section of the vertical tail. This pressure on the horizontal tail induced by the vertical tail gives rise to the rolling-moment contribution of the horizontal tail. For positive sideslip (positive angle of attack), the perturbation flow over the right-side surface (outward normal to surface in direction of positive y-axis) of the vertical tail induces a downward force on the right panel of the horizontal tail and, similarly, the perturbation flow over the left-side surface of the vertical tail induces an equivalent upward force on the left panel of the horizontal tail. For sideslip, the rolling-moment contributions about the body axes of the vertical and horizontal tail are of opposite signs and tend to counteract each other. The quantity $\left(C_{l_\beta}\right)_{ht}$ was found by integration and is given by the following expression for an arbitrary taper ratio (including a taper ratio of 1):

$$
\begin{aligned}
\left(C_{l_\beta}\right)_{ht} = {} & \frac{-4c_r{}^3 m_0{}^2 m'}{8_V b_V 3\pi B \sqrt{m'^2 - 1}} \cdot \left\{ \frac{B^2 m_0{}^2 \sqrt{m'^2 - 1}}{\left(B^2 m_0{}^2 - 1\right)\left[m'^2 - B^2 m_0{}^2(m'^2 - 1)\right]} + \frac{m'^2 \pi}{2\left(m' - B m_0 \sqrt{m'^2 - 1}\right)^2} + \right. \\[2ex]
& \frac{B^2 m_0{}^2 \sqrt{m'^2 - 1}\left[B^2 m_0{}^2 - 3m'^2(B^2 m_0{}^2 - 1)\right]}{\sqrt{B^2 m_0{}^2 - 1}\,(B^2 m_0{}^2 - 1)\left[m'^2 - B^2 m_0{}^2(m'^2 - 1)\right]^2}\left(\sin^{-1}\frac{1}{B m_0} + \frac{\pi}{2}\right) - \\[2ex]
& \left. \frac{m'^2\left[m'^2 + B^2 m_0{}^2(m'^2 - 1)\right]}{\left[m'^2 - B^2 m_0{}^2(m'^2 - 1)\right]^2}\cos^{-1}\frac{\sqrt{m'^2 - 1}}{m'} \right\}
\end{aligned}
\qquad (31)
$$

The results for the rolling-moment derivative were given relative to a system of body axes located at the leading edge of the root section. (See fig. 2.) The transformation formula for conversion of the rolling-moment derivative from body axes to stability axes is given in reference 7. The rolling-moment derivative about the stability axes based upon wing area and wing span is given by

$$C_{l_\beta}{}' = \frac{b_v S_v}{b_w S_w}\left[\left(C_{l_\beta}\right)_t + \alpha\left(C_{n_\beta}\right)_t\right] \tag{32}$$

when only first-order terms in α are retained.

The end-plate effect of the horizontal tail on the derivative $\left(C_{l_\beta}\right)_t$ is made up of three effects: The change in $\left(C_{Y_\beta}\right)_t$, the change in the distance $\bar{Z}$, and the change in the rolling moment due to the horizontal tail $\left(C_{l_\beta}\right)_{ht}$. The change in $\left(C_{Y_\beta}\right)_t$ and the change in the rolling moment due to the horizontal tail have already been evaluated; hence, only the change in the distance $\bar{Z}$ remains to be evaluated. This change $\Delta\bar{Z}$ in the center-of-pressure distance $\bar{Z}$ can be written mathematically as

$$\Delta\bar{Z} = \frac{\bar{Z}\left(C_{Y_\beta}\right)_t + b_v\Delta\left(C_{l_\beta}\right)_{vt}}{\left(C_{Y_\beta}\right)_t + \Delta\left(C_{Y_\beta}\right)_t} - \bar{Z} \tag{33}$$

where $\Delta\left(C_{l_\beta}\right)_{vt}$ is the change in the rolling moment due to the vertical tail. The quantity $\Delta\left(C_{l_\beta}\right)_{vt}$ was found by integration and is given by the following equations:

For an arbitrary taper ratio,

$$\Delta\left(C_{l_\beta}\right)_{vt} = \frac{32m'^3K^2}{\pi J^2(1+\lambda)\sqrt{m'^2-1}}\left[\frac{1+K^2}{3(1-K^2)^2}\cos^{-1}\frac{1}{m'} - \frac{K^2\sqrt{m'^2-1}}{3(1-K^2)(K^2m'^2-1)} + \right.$$

$$\frac{K\sqrt{m'^2-1}(-3K+2K^3m'^2+K^3)}{3\sqrt{m'K+1}(1-K^2)^2(m'^2K^2-1)\sqrt{m'K-1}}\cos^{-1}\frac{-1}{Km'} +$$

$$\left.\frac{\pi\sqrt{m'-1}(-2K^3m'^2+5K^2m'-K^3m'+K^2-3K)}{12(m'K-1)^2(1-K)^2\sqrt{K}\sqrt{Km'-1}}\right] \tag{34}$$

For a taper ratio of 1,

$$\Delta\left(C_{l_\beta}\right)_{vt} = \frac{m'^3}{3\pi BA'^2}\left[\frac{m'^4 - 2m'^2 + 4}{(m'^2 - 1)^2\sqrt{m'^2 - 1}}\cos^{-1}\frac{1}{m'} + \right.$$

$$\left.\frac{m'^2 - 4}{(m'^2 - 1)^2} + \frac{\pi(-2m'^4 + 7m'^2 + 6m' - 11)}{4(m'^2 - 1)^2\sqrt{m'^2 - 1}}\right] \qquad (35)$$

Equation (26) indicates that the derivative $\left(C_{l_\beta}\right)_t$ can be expressed in terms of the derivative $\left(C_{Y_\beta}\right)_t$, an arm $\bar{Z}$, and a moment due to the horizontal tail. Figure 12 shows calculated values of the arm $\bar{Z}$ for taper ratios of 0 and 1. The dashed parts of the curves of figure 12 are faired since formulas were not found for this region. Figure 13 shows calculated values from which the moment due to the load on the horizontal tail may be evaluated.

The change in the distance $\bar{Z}$ due to the horizontal tail was calculated for taper ratios of 0 and 1 for various values of sweep angle, Mach number, and aspect ratio. These calculated data are presented in figure 14. Figure 15 presents some illustrative variations of the derivative C_{l_β}' with and without the horizontal tail for various values of Mach number, aspect ratio, and sweep angle.

DISCUSSION

The calculated results for the derivatives of the combination of the vertical and horizontal tails show the expected trends; however, a few results concerning the end-plate effect of the horizontal tail may warrant discussion. Figures 6 and 7 indicate that maximum decrease in $\left(C_{Y_\beta}\right)_t$ due to removal of the horizontal tail is from 25 to 30 percent of the value of $\left(C_{Y_\beta}\right)_t$. This maximum appears to occur at a taper ratio of 0 for low values of the parameter BA. From this maximum the end-plate effect decreases to values which are negligible compared to the values of $\left(C_{Y_\beta}\right)_t$ for large values of the parameter BA. The effect of the horizontal tail on the derivative $\left(C_{n_\beta}\right)_t$ depends on $\Delta\left(C_{Y_\beta}\right)_t$ and on the length of the arm $\left(l_t + \bar{X}\right)$. Generally, the length l_t is somewhat larger than the length $\bar{X}$; therefore the change in $\bar{X}$ due to

the horizontal tail has a small effect on the arm $\left(l_t + \bar{X}\right)$. In these cases the effect of the horizontal tail on the derivative $\left(C_{n_\beta}\right)_t$ has the same trends as those of the derivative $\left(C_{Y_\beta}\right)_t$. The end-plate effect of the horizontal tail on the derivative $\left(C_{l_\beta}\right)_t$ is made up of the change in the distance $\bar{Z}$, the change in the lateral force $\Delta\left(C_{Y_\beta}\right)_t$, and the rolling moment due to the horizontal tail. The rolling moment caused by the load on the horizontal tail opposes the rolling moment due to the load on the vertical tail so that it is possible for $\left(C_{l_\beta}\right)_t$ to be increased or decreased by removing the horizontal tail. This effect is shown in figure 15(b) or 15(c).

PROCEDURE FOR CALCULATION OF STABILITY DERIVATIVES C_{Y_β}, C_{l_β},

AND C_{n_β} FOR GIVEN TAIL ARRANGEMENT AND MACH NUMBER

The results of the preceding analysis of the sideslip derivatives may not be conveniently presented in a form from which values of the derivative can be directly obtained. The purpose of this section is to set forth in detail a procedure for the calculation of the stability derivatives for a given tail arrangement and Mach number.

The proper use of the formulas derived in the previous section requires the following consideration of the radical sign. The radical sign $\sqrt{}$ is defined as the positive root of the quantity under the radical; thus if a is a positive number,

$$\sqrt{(\pm a)^2} = a$$

However, note that

$$\sqrt{-a}\,\sqrt{-a} = i\,\sqrt{a}\,\,i\,\sqrt{a} = -a \neq \sqrt{(-a)(-a)}$$

Lateral-Force Coefficient for Vertical

Tail in Presence of Horizontal Tail

The derivative $\left(C_{Y_\beta}\right)_t$ may be determined as follows. First, the products BA and Bm are evaluated. The second step depends upon the value of the taper ratio of the vertical tail together with the degree

of accuracy desired. If the taper ratio of the vertical tail is 0, 1/2, or 1 the value of $\left(C_{Y_\beta}\right)_t$ may be obtained directly from figure 6. If the value of the taper ratio is not 0, 1/2, or 1 and if extreme accuracy is not desired the values of $\left(C_{Y_\beta}\right)_t$ may still be determined from figure 6 by interpolation. If greater accuracy is desired the position of the Mach lines on the vertical tail must be determined. The values of $\left(C_{Y_\beta}\right)_t$ may then be evaluated from equations (2), (4), (6), (8), or (9) depending on the plan form of the vertical tail and on the Mach line configuration. The conversion of the lateral-force coefficient from body axes to stability axes and the conversion from a coefficient based on the vertical-tail area to a coefficient based on the wing area is given by the expression

$$C_{Y_\beta}{}' = \frac{S_V}{S_W} \left(C_{Y_\beta}\right)_t$$

Lateral-Force Coefficient $\left(C_{Y_\beta}\right)_V$ of Isolated Vertical Tail

The lateral-force coefficient for a vertical-tail alone $\left(C_{Y_\beta}\right)_V$ may be determined for the case where the Mach line from the center section cuts the trailing edge of the vertical tail. The lateral-force coefficient is given by $\left(C_{Y_\beta}\right)_V = \left(C_{Y_\beta}\right)_t + \Delta\left(C_{Y_\beta}\right)_t$. The procedure for evaluating $\left(C_{Y_\beta}\right)_t$ has been discussed previously. The procedure for evaluating $\Delta\left(C_{Y_\beta}\right)_t$ is as follows. For taper ratios of 0, 1/2, or 1 the values of $\Delta\left(C_{Y_\beta}\right)_t$ may be found from figure 7; if, however, the taper ratio is not 0, 1/2, or 1, good approximations to the value of $\Delta\left(C_{Y_\beta}\right)_t$ may be determined from figure 7 by interpolation. If greater accuracy is desired, the value of $\Delta\left(C_{Y_\beta}\right)_t$ must be calculated from equations (10), (12), or (13) depending on the plan form under consideration. The conversion of the lateral-force derivative for a vertical tail alone from body axes to stability axes including the conversion of the derivative based on the wing area is given by the formula

$$C_{Y_\beta}{}' = \frac{S_V}{S_W}\left(C_{Y_\beta}\right)_V = \frac{S_V}{S_W}\left[\left(C_{Y_\beta}\right)_t + \Delta\left(C_{Y_\beta}\right)_t\right]$$

Yawing-Moment Coefficient for Vertical Tail in

Presence of Horizontal Tail

The derivative $\left(C_{n_\beta}\right)_t$ may be expressed in terms of the quantities l_t/b_V, $\left(C_{Y_\beta}\right)_t$, and $\overline{X}/b_V$ as follows:

$$\left(C_{n_\beta}\right)_t = \left(C_{Y_\beta}\right)_t\left(\frac{\overline{X}}{b_V} + \frac{l_t}{b_V}\right)$$

The geometric quantity l_t/b_V is known. The procedure for finding the quantity $\left(C_{Y_\beta}\right)_t$ has been given previously. The evaluation of the quantity $\overline{X}/b_V$ may be determined as follows. First, of course, the products BA and Bm are evaluated. The next step depends upon the value of the taper ratio of the vertical tail. For vertical tails which have a taper ratio of 0 or 1, $\overline{X}/b_V$ can be obtained directly from figure 9. If the taper ratio of the vertical tail is not 0 or 1, interpolation may be used to obtain $\overline{X}/b_V$ if the degree of accuracy desired is not great. When greater accuracy is desired the procedure to be followed depends upon the Mach line configuration of the vertical tail. If the Mach line from the root section cuts the trailing edge, $\overline{X}/b_V$ may be evaluated from equation (17). For the cases where the Mach line from the root section is coincident with the leading edge, $\overline{X}/b_V$ can be evaluated from equation (15). If the Mach line from the root section cuts the tip, $\overline{X}/b_V$ cannot be directly evaluated; it can be approximated however, by interpolation between the values of $\overline{X}/b_V$ for the case where the Mach line from the root section is coincident with the leading edge of the vertical tail and for the case where the Mach line from the root section cuts the trailing edge.

The conversion of the yawing-moment coefficient for a vertical tail in the presence of a horizontal tail from body axes to stability axes (including the change in the coefficient so that it is based on the wing area and span) is given by

$$C_{n_\beta}' = \frac{b_V S_V}{b_W S_W}\left[\left(C_{n_\beta}\right)_t - \alpha\left(C_{l_\beta}\right)_t\right]$$

where α, of course, is assumed to be small.

Yawing-Moment Coefficient for Vertical Tail Alone

The yawing-moment coefficient for a vertical tail alone $\left(C_{n_\beta}\right)_v$ was investigated for the case where the Mach line from the root section cuts the trailing edge. This derivative can be expressed as

$$\left(C_{n_\beta}\right)_v = \left[\left(C_{Y_\beta}\right)_t + \Delta\left(C_{Y_\beta}\right)_t\right]\left(\frac{\overline{X}}{b_v} + \frac{\Delta\overline{X}}{b_v} + \frac{l_t}{b_v}\right) = \left(C_{Y_\beta}\right)_v\left(\frac{\overline{X}}{b_v} + \frac{\Delta\overline{X}}{b_v} + \frac{l_t}{b_v}\right)$$

The procedure for evaluating the quantity $\left(C_{Y_\beta}\right)_v$ has been given previously. Once the products Bm and BA are evaluated, the quantity $\Delta\overline{X}/b_v$ may be found directly from figure 14 for taper ratios of 0 and 1. For other taper ratios between 0 and 1 the quantity $\Delta\overline{X}/b_v$ can be estimated by interpolation by use of figure 14.

If greater accuracy is desired in the evaluation of $\left(C_{n_\beta}\right)_v$, the following procedure may be used. The derivative $\left(C_{n_\beta}\right)_v$ can be expressed as

$$\left(C_{n_\beta}\right)_v = \left(C_{n_\beta}\right)_t + \Delta\left(C_{n_\beta}\right)_t$$

The method for calculating the quantity $\left(C_{n_\beta}\right)_t$ has been set forth previously. The quantity $\Delta\left(C_{n_\beta}\right)_t$ can be evaluated from equation (21).

The conversion of the yawing-moment coefficient for a vertical tail alone from body axes to stability axes and from a coefficient based on the vertical-tail area and span to a coefficient based on the wing area and span is given by

$$C_{n_\beta}' = \frac{S_v b_v}{S_w b_w}\left[\left(C_{n_\beta}\right)_v - \alpha\left(C_{l_\beta}\right)_v\right]$$

where α is assumed to be small.

Rolling-Moment Coefficient for Vertical-Tail

and Horizontal-Tail Combination

The rolling-moment coefficient for the vertical-tail and horizontal-tail combination $\left(C_{l_\beta}\right)_t$ can be expressed as

$$\left(C_{l_\beta}\right)_t = \left(C_{l_\beta}\right)_{vt} + \left(C_{l_\beta}\right)_{ht} = \left(C_{Y_\beta}\right)_t \frac{\overline{Z}}{b_V} + \left(C_{l_\beta}\right)_{ht}$$

The procedure for finding the quantity $\left(C_{Y_\beta}\right)_t$ has been considered previously. Once the products Bm and AB are evaluated $\overline{Z}/b_V$ may be found from figure 12 for taper ratios of 0 and 1. If the taper ratio of the vertical tail is not 0 or 1, approximate values of $\overline{Z}/b_V$ can be obtained by interpolation. For accurate evaluations, the Mach line configuration on the vertical tail must be determined. For cases where the Mach line from the root section is coincident with the leading edge of the vertical tail, values of $\overline{Z}/b_V$ can be found from equation (28). For cases where the Mach lines from the root section cut the trailing edge, values of $\overline{Z}/b_V$ can be found from equation (29). If the Mach line from the root section cuts the tip, $\overline{Z}/b_V$ can only be approximately evaluated by interpolating between the values of $\overline{Z}/b_V$ for the condition where the Mach line from the root section is coincident with the leading edge of the vertical tail and for the condition where the Mach line from the root section just cuts the trailing edge.

The quantity $\left(C_{l_\beta}\right)_{ht}$ was investigated for a horizontal-tail plan form for which the trailing edge is swept at a constant angle, for Mach numbers for which the Mach line from the root section cuts the trailing edge of the horizontal tail, and where the Mach cone from the leading edge of the tip section of the vertical tail does not intersect the horizontal tail. For this case, the quantity $\left(C_{l_\beta}\right)_{ht}$ can be found with the use of figure 13 or it may be calculated from equation (31).

The conversion of the rolling-moment derivative for the vertical-tail and horizontal-tail combination from body axes to stability axes (including a change in the derivative so that it is based upon the wing area and wing span) is given by

$$C_{l_\beta}' = \frac{b_V S_V}{b_W S_W}\left[\left(C_{l_\beta}\right)_t + \alpha\left(C_{n_\beta}\right)_t\right]$$

where α is assumed to be small.

Rolling-Moment Coefficient for Vertical Tail Alone

The rolling-moment coefficient for vertical tail alone $\left(C_{l_\beta}\right)_v$ was investigated for the case where the Mach line from the root section cuts the trailing edge of the vertical tail. The derivative $\left(C_{l_\beta}\right)_v$ can be expressed as

$$\left(C_{l_\beta}\right)_v = \left(C_{Y_\beta}\right)_v\left(\frac{\overline{Z}}{b_V} + \frac{\Delta\overline{Z}}{b_V}\right) \tag{36}$$

or

$$\left(C_{l_\beta}\right)_v = \left(C_{l_\beta}\right)_{vt} + \Delta\left(C_{l_\beta}\right)_{vt} \tag{37}$$

The procedure for the determination of $\left(C_{Y_\beta}\right)_v$, $\overline{Z}/b_V$, and $\left(C_{l_\beta}\right)_{vt}$ has been given previously. For taper ratios of 0 or 1 the quantity $\Delta\overline{Z}/b_V$ can be found directly from figure 14. Thus, $\left(C_{l_\beta}\right)_v$ can be found from equation (36). If the taper ratio is not 0 or 1 the value of $\Delta\overline{Z}/b_V$ may be estimated from figure 14 by interpolation. For precise evaluations, the quantity $\Delta\left(C_{l_\beta}\right)_{vt}$ may be evaluated from equation (34). Thus, $\left(C_{l_\beta}\right)_v$ can be found from equation (37).

The conversion of the rolling-moment coefficient for a vertical tail alone from body axes to stability axes and from a coefficient based on the vertical-tail area and span to a coefficient based on the wing area and span is given by

$$C_{l_\beta}' = \frac{S_V b_V}{S_W b_W}\left[\left(C_{l_\beta}\right)_v + \alpha\left(C_{n_\beta}\right)_v\right]$$

where α is assumed to be small.

CONCLUDING REMARKS

The linearized theory has enabled an evaluation of a first approximation to the lateral force due to sideslip C_{Y_β}, the yawing moment due to sideslip C_{n_β}, and the rolling moment due to sideslip C_{l_β} for a

number of tail configurations. The influence of the wing on these tail derivatives has not been considered.

The suitability of the results for full-scale flight stability calculations is necessarily limited because of the restrictions of the linearized potential-flow theory.

Langley Aeronautical Laboratory
        National Advisory Committee for Aeronautics
                Langley Field, Va., February 2, 1951

REFERENCES

1. Jones, Arthur L: The Theoretical Lateral-Stability Derivatives for Wings at Supersonic Speeds. Jour. Aero. Sci., vol. 17, no. 1, Jan. 1950, pp. 39-46.

2. Campbell, John P., and McKinney, Marion O.: Summary of Methods for Calculating Dynamic Lateral Stability and Response and for Estimating Lateral Stability Derivatives. NACA TN 2409, 1951.

3. Harmon, Sidney M., and Jeffreys, Isabella: Theoretical Lift and Damping in Roll of Thin Wings with Arbitrary Sweep and Taper at Supersonic Speeds. Supersonic Leading and Trailing Edges. NACA TN 2114, 1950.

4. Puckett, Allen E.: Supersonic Wave Drag of Thin Airfoils. Jour. Aero. Sci., vol. 13, no. 9, Sept. 1946, pp. 475-484.

5. Evvard, John C.: Distribution of Wave Drag and Lift in the Vicinity of Wing Tips at Supersonic Speeds. NACA TN 1382, 1947.

6. Lagerstrom, P. A., Wall, D., and Graham, M. E.: Formulas in Three-Dimensional Wing Theory. Rep. No. SM-11901, Douglas Aircraft Co., Inc., July 8, 1946.

7. Glauert, H.: A Non-Dimensional Form of the Stability Equations of an Airplane. R. & M. No. 1093, British A.R.C., 1927.

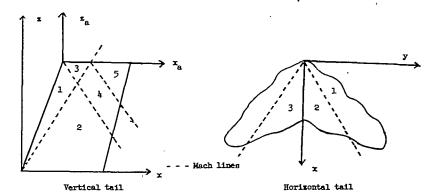TABLE I.- FORMULAS FOR POTENTIAL DISTRIBUTION DUE TO SIDESLIP

--- Mach lines

Vertical tail   Horizontal tail

Region (see sketches)	Vertical tail with horizontal tail, $\phi(x,0^+,z)$
1	$-\dfrac{v\beta(mx - z)}{\sqrt{B^2m^2 - 1}}$
2	$-\dfrac{v\beta}{\pi\sqrt{B^2m^2 - 1}}\left[(mx - z)\cos^{-1}\dfrac{z - B^2mx}{B(mx - z)} + (mx + z)\cos^{-1}\dfrac{z + B^2mx}{B(mx + z)}\right]$
3	$-\dfrac{v\beta}{\pi\sqrt{B^2m^2 - 1}}\left[(mx_a - z_a)\cos^{-1}\dfrac{mx_a + z_a(2Bm + 1)}{mx_a - z_a} + 2\sqrt{-mz_a(x_a + Bz_a)(Bm + 1)}\right]$
4	$-\dfrac{v\beta}{\pi\sqrt{B^2m^2 - 1}}\left\{(mx_a - z_a)\left[\cos^{-1}\dfrac{mx_a + z_a(2Bm + 1)}{mx_a - z_a} - \cos^{-1}\dfrac{-mx_a + B^2m^2z_a + b_v(B^2m^2 - 1)}{Bm(mx_a - z_a)}\right] + \right.$ $\left. (mx_a + 2b_v + z_a)\cos^{-1}\dfrac{mx_a + B^2m^2z_a + b_v(B^2m^2 + 1)}{Bm(mx_a + z_a + 2b_v)} + 2\sqrt{-mz_a(x_a + Bz_a)(Bm + 1)}\right\}$
5	$-\dfrac{v\beta}{\pi\sqrt{B^2m^2 - 1}}\left[(mx_a + z_a + 2b_v)\cos^{-1}\dfrac{mx_a + z_a(2Bm - 1) + 2b_v}{mx_a + z_a + 2b_v} + 2\sqrt{-z_a(mx_a + Bmz_a + 2b_v)(Bm - 1)}\right]$

Region	Vertical tail without horizontal tail, $\phi(x,0^+,z)$
1	$-\dfrac{v\beta(mx - z)}{\sqrt{B^2m^2 - 1}}$
2	$-\dfrac{v\beta}{\pi\sqrt{B^2m^2 - 1}}\left[(mx - z)\cos^{-1}\dfrac{mx - z(2Bm - 1)}{(mx - z)} + 2\sqrt{zm(x - Bz)(Bm - 1)}\right]$
3	$-\dfrac{v\beta}{\pi\sqrt{B^2m^2 - 1}}\left[(mx_a - z_a)\cos^{-1}\dfrac{mx_a + z_a(2Bm + 1)}{mx_a - z_a} + 2\sqrt{-mz_a(x_a + Bz_a)(Bm + 1)}\right]$
4	$-\dfrac{v\beta}{\pi\sqrt{B^2m^2 - 1}}\left\{(mx_a - z_a)\left[\cos^{-1}\dfrac{mx_a + z_a(2Bm + 1)}{mx_a - z_a} - \cos^{-1}\dfrac{z_a(2Bm - 1) + 2b_v(Bm - 1) - mx_a}{mx_a - z_a}\right] + \right.$ $\left. 2\sqrt{(z_a + b_v)[mx_a + b_v - Bm(z_a - b_v)](Bm - 1)} + 2\sqrt{-z_a m(x_a + Bz_a)(Bm + 1)}\right\}$

Region	Upper surface of horizontal tail, $\phi(x,y,0^+)$
1	0
2	$\dfrac{-v\beta}{\pi\sqrt{B^2m^2 - 1}}\left[mx\cos^{-1}\dfrac{(2 - m^2B^2)x^2 + B^2y^2(B^2m^2 - 1)}{B^2m^2x^2 - B^2y^2(B^2m^2 - 1)} - By\sqrt{B^2m^2 - 1}\cos^{-1}\dfrac{B^2x^2(B^2m^2 + 1) - B^2m^2x^2}{B^2m^2x^2 - B^2y^2(B^2m^2 - 1)}\right]$
3	$\dfrac{v\beta}{\pi\sqrt{B^2m^2 - 1}}\left[mx\cos^{-1}\dfrac{(2 - m^2B^2)x^2 + B^2y^2(B^2m^2 - 1)}{B^2m^2x^2 - B^2y^2(B^2m^2 - 1)} - By\sqrt{B^2m^2 - 1}\cos^{-1}\dfrac{B^2y^2(B^2m^2 + 1) - B^2m^2x^2}{B^2m^2x^2 - B^2y^2(B^2m^2 - 1)}\right]$

TABLE II.- FORMULAS FOR PRESSURE-DIFFERENCE COEFFICIENT DUE TO SIDESLIP

Vertical tail   Horizontal tail

Region (see sketches)	Vertical tail with horizontal tail
1	$-\dfrac{4\beta m}{\sqrt{B^2 m^2 - 1}}$
2	$-\dfrac{4\beta m}{x\sqrt{B^2 m^2 - 1}}\left[\cos^{-1}\dfrac{x - B^2 mz}{B(mx - z)} + \cos^{-1}\dfrac{x + B^2 mz}{B(mx + z)}\right]$
3	$-\dfrac{4\beta m}{\pi\sqrt{B^2 m^2 - 1}}\cos^{-1}\dfrac{mx_a + z_a(2Bm + 1)}{mx_a - z_a}$
4	$-\dfrac{4\beta m}{x\sqrt{B^2 m^2 - 1}}\left[-\cos^{-1}\dfrac{-\left[mx_a + z_a(2Bm + 1)\right]}{mx_a - z_a} + \cos^{-1}\dfrac{mx_a - B^2 m^2 z_a - \left(B^2 m^2 - 1\right)b_v}{Bm(mx_a - z_a)} + \cos^{-1}\dfrac{mx_a + B^2 m^2 z_a + b_v\left(B^2 m^2 + 1\right)}{Bm\left(mx_a + 2b_v + z_a\right)}\right]$
5	$-\dfrac{4\beta m}{x\sqrt{B^2 m^2 - 1}}\cos^{-1}\dfrac{mx_a - z_a(1 - 2Bm) + 2b_v}{mx_a + z_a + 2b_v}$

	Vertical tail without horizontal tail
1	$-\dfrac{4\beta m}{\sqrt{B^2 m^2 - 1}}$
2	$-\dfrac{4\beta m}{\pi\sqrt{B^2 m^2 - 1}}\cos^{-1}\dfrac{mx - z(2Bm - 1)}{mx - z}$
3	$-\dfrac{4\beta m}{x\sqrt{B^2 m^2 - 1}}\cos^{-1}\dfrac{mx_a + z_a(2Bm + 1)}{mx_a - z_a}$
4	$\dfrac{-4\beta m}{\pi\sqrt{B^2 m^2 - 1}}\left[\cos^{-1}\dfrac{mx_a + z_a(2Bm + 1)}{mx_a - z_a} - \cos^{-1}\dfrac{-\left[mx_a - z_a(2Bm - 1) - 2b_v(Bm - 1)\right]}{mx_a - z_a}\right]$

	Horizontal tail
1	0
2	$-\dfrac{4\beta m}{\pi\sqrt{B^2 m^2 - 1}}\cos^{-1}\dfrac{x}{\sqrt{B^2 m^2 x^2 - y^2 B^2\left(B^2 m^2 - 1\right)}}$
3	$\dfrac{4\beta m}{x\sqrt{B^2 m^2 - 1}}\cos^{-1}\dfrac{x}{\sqrt{B^2 m^2 x^2 - y^2 B^2\left(B^2 m^2 - 1\right)}}$

(a) Taper ratio, I.

(b) Taper ratio, O.

(c) Arbitrary taper ratio.
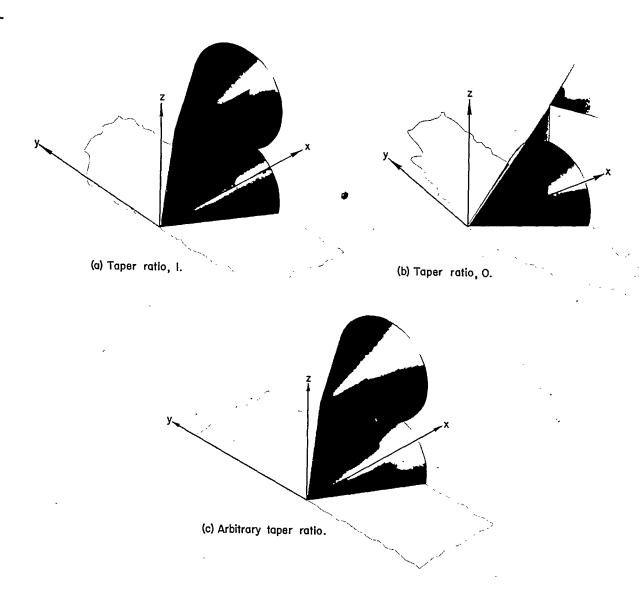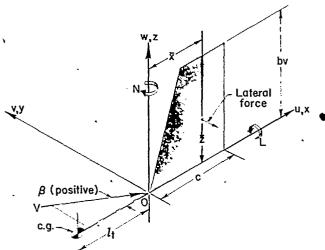
Figure 1.- Types of vertical tails treated.   L-67012

(a) Notation and body axes
used in analysis.

(b) Stability axes (body axes dashed).
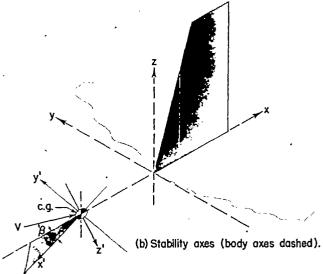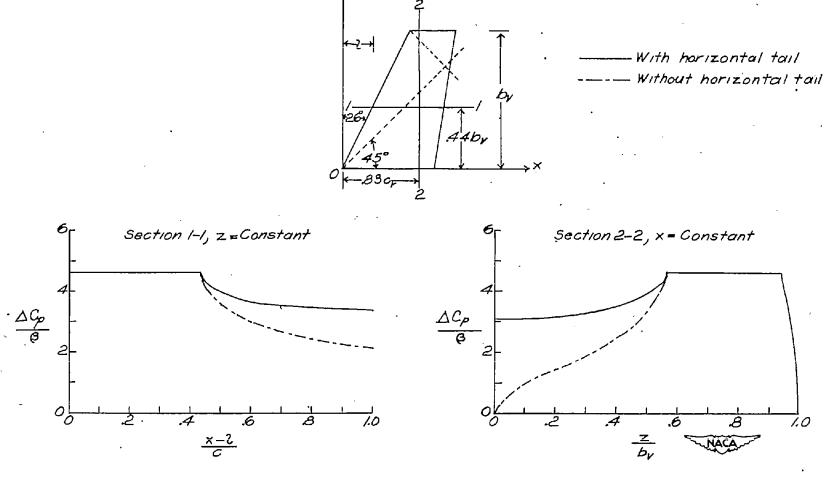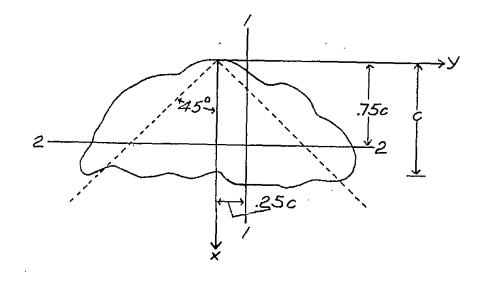
Figure 2.- Systems of axes.   L-67013.1

Figure 3.- Chordwise and spanwise pressure distributions on the vertical tail with $B = 1$, $m = 2.05$, and $\lambda = 0.5$.
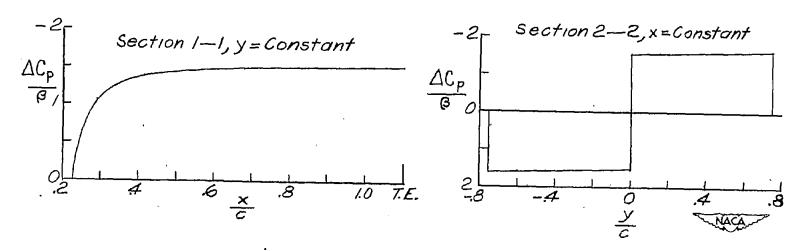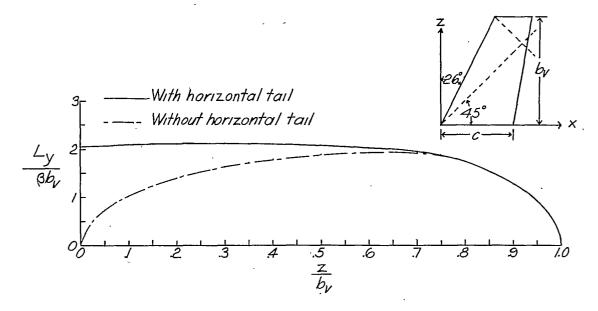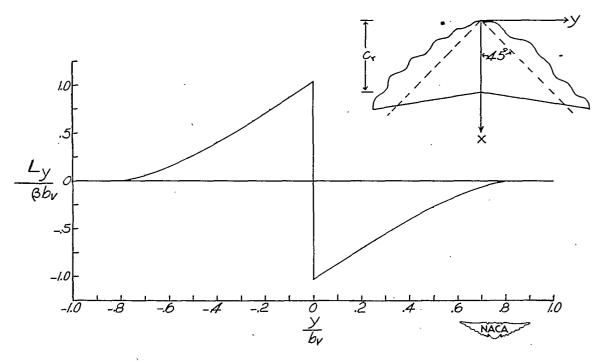
Figure 4.- Chordwise and spanwise pressure distributions on the horizontal tail with B = 1 and m = 2.05.
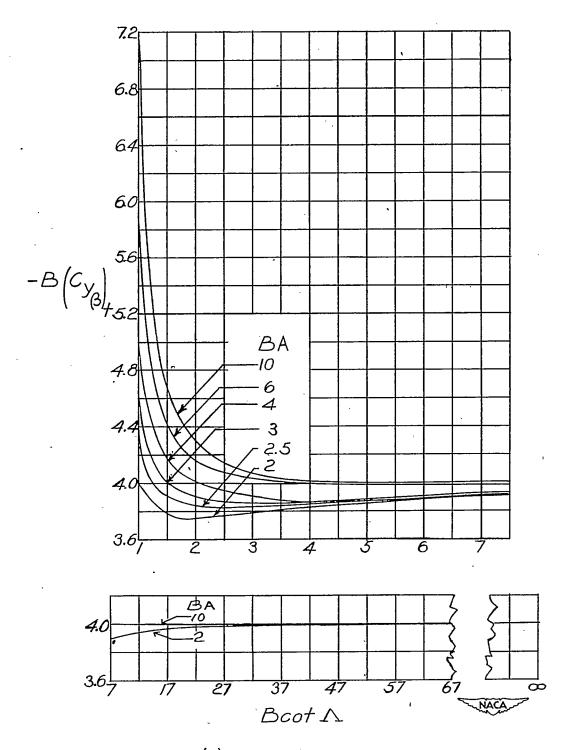
(a) Vertical tail.
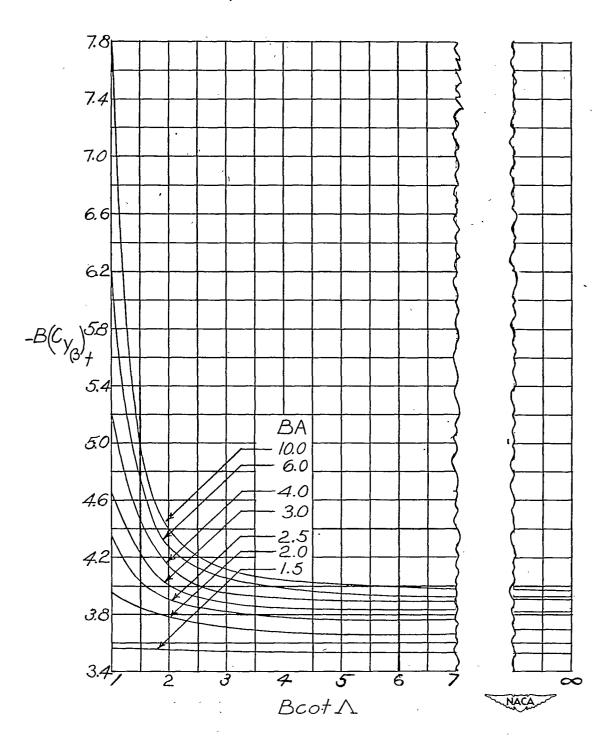
(b) Horizontal tail.

Figure 5.- Spanwise loading for vertical and horizontal tails with B = 1,
A = 2,   m = 2, λ = 0.5, and m_0 = 6.
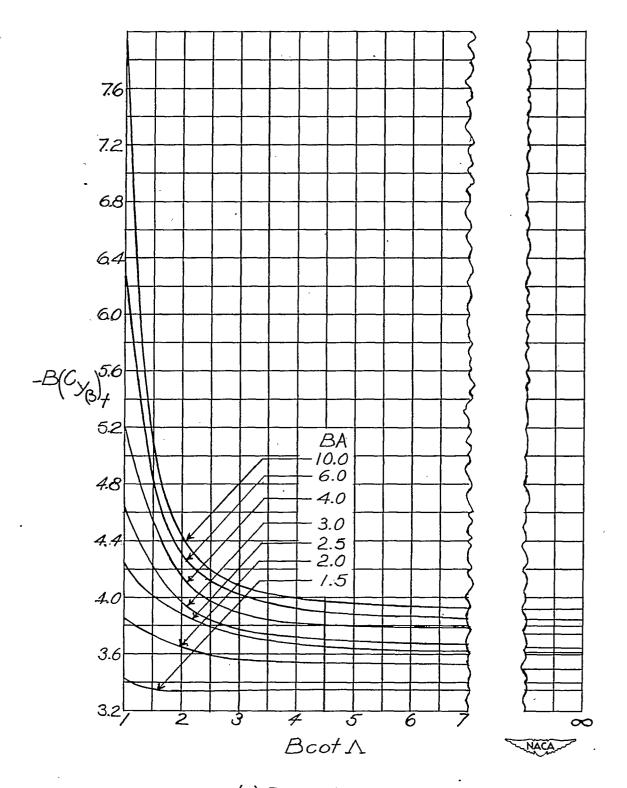
(a) Taper ratio of 0.

Figure 6.- Variation of $-B\left(C_{Y_\beta}\right)_t$ with sweepback-angle parameter for various values of aspect-ratio parameter and taper ratio. (Data taken from reference 2.)

(b) Taper ratio of 1/2.

Figure 6.- Continued.

$-B\left(C_{y_\beta}\right)_{\ddagger}$

$B cot \Lambda$

(c) Taper ratio of 1.

Figure 6.- Concluded.
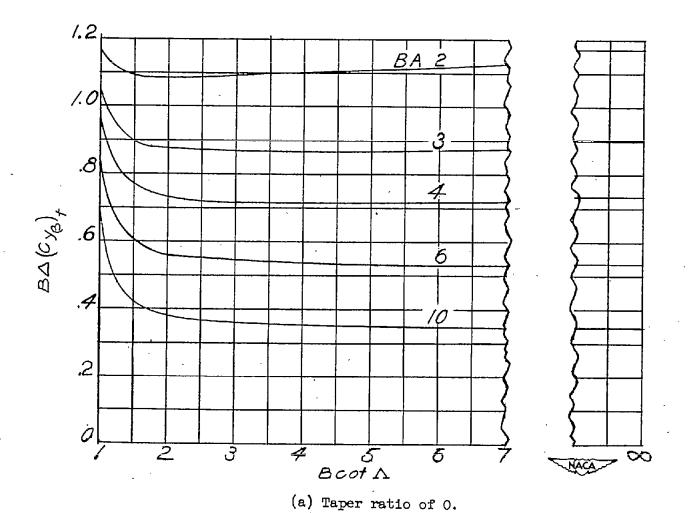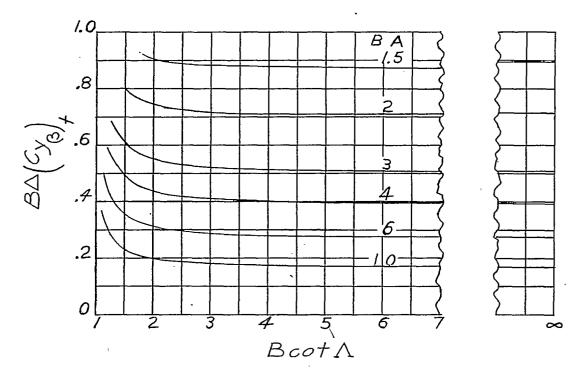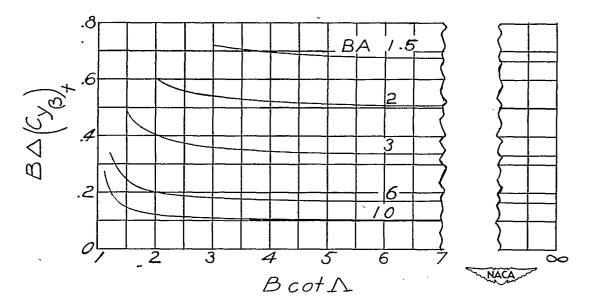
(a) Taper ratio of 0.

Figure 7.- Variation of $B \Delta\left(C_{Y_\beta}\right)_t$ due to the horizontal tail with sweepback-angle parameter for various values of aspect-ratio parameter and taper ratio.
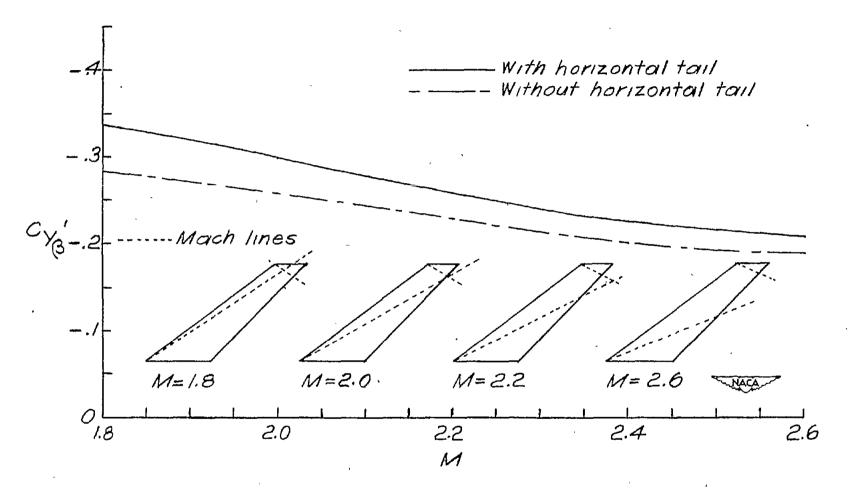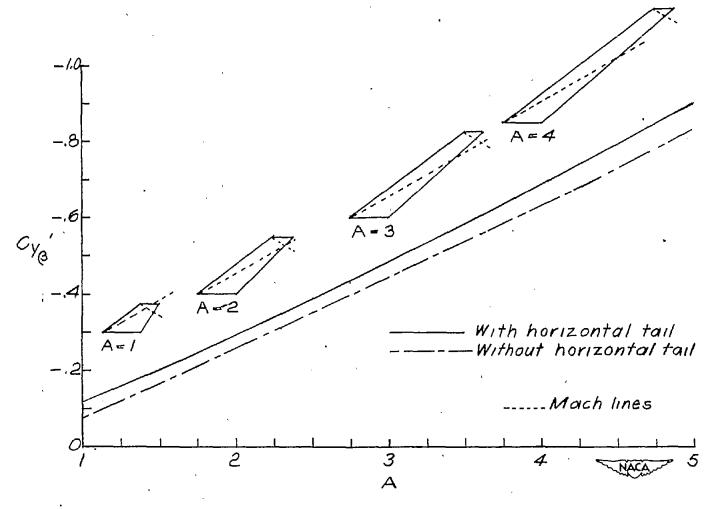
(b) Taper ratio of 1/2.

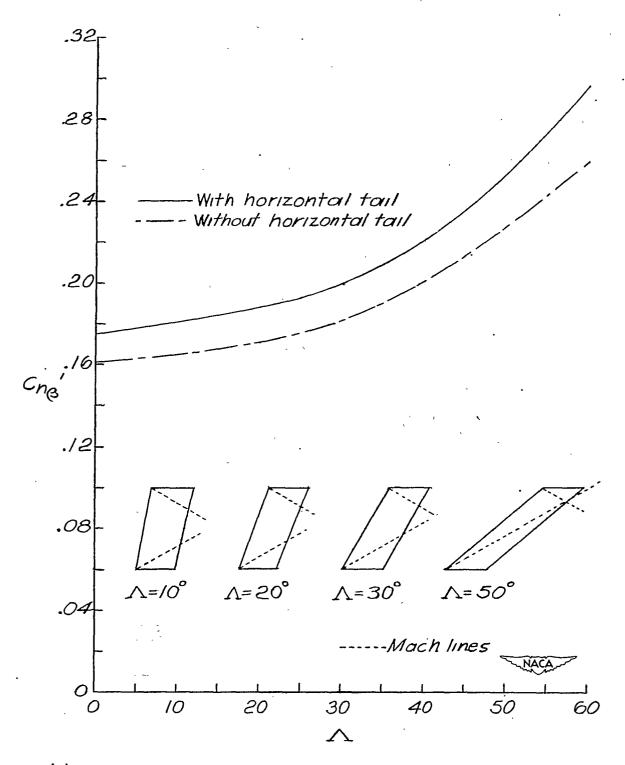
(c) Taper ratio of 1.

Figure 7.- Concluded.
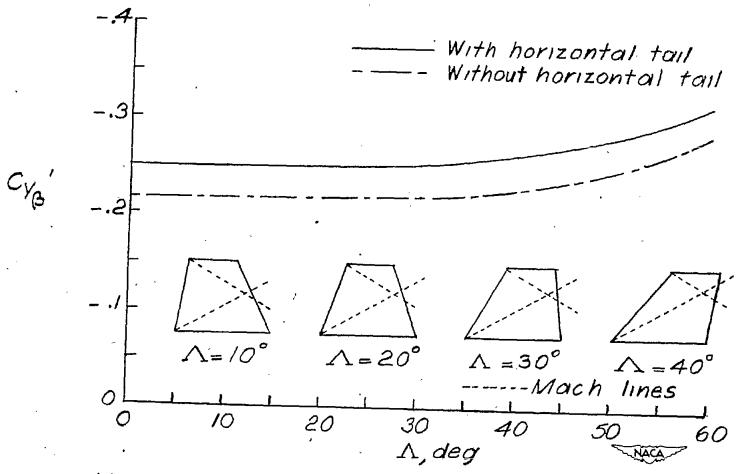
(a) Illustrative variation with Mach number. $A = 2$; $\lambda = 0.5$; $\Lambda = 53°$.
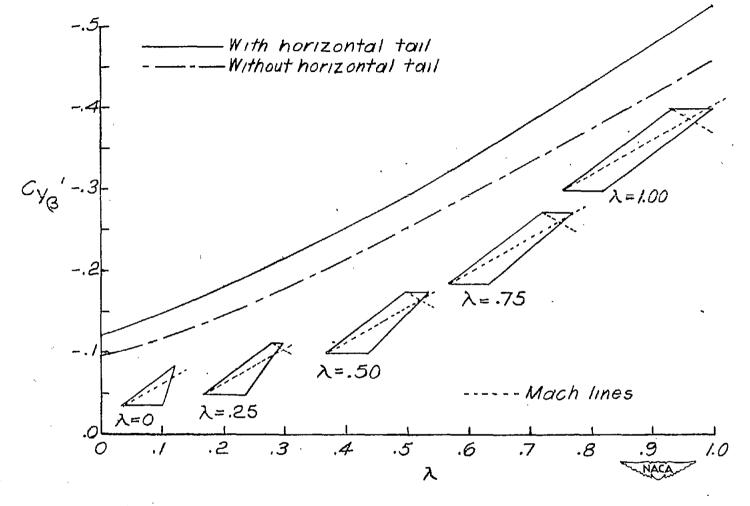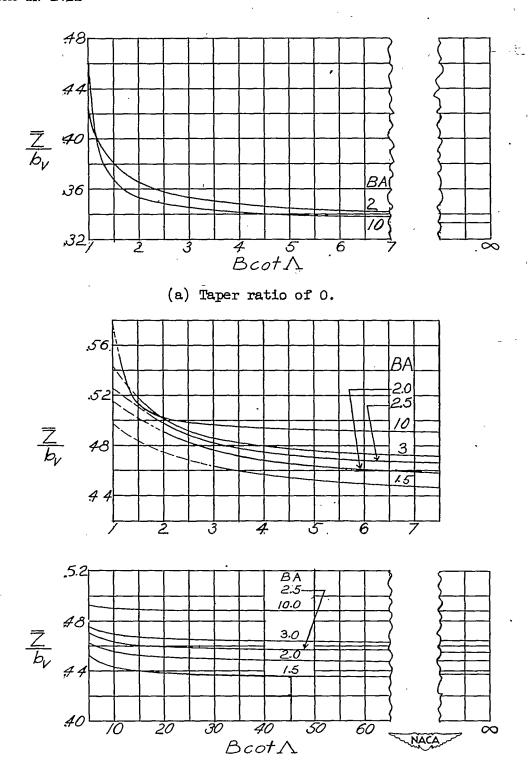
Figure 8.- Some illustrative variations of C_{Y_β}' with Mach number, aspect ratio, sweep angle, and taper ratio for $\dfrac{S_w}{c_r^2} = 10$.

(b) Illustrative variation with aspect ratio. M = 2; λ = 0.5; Λ = 53°.

Figure 8.- Continued.
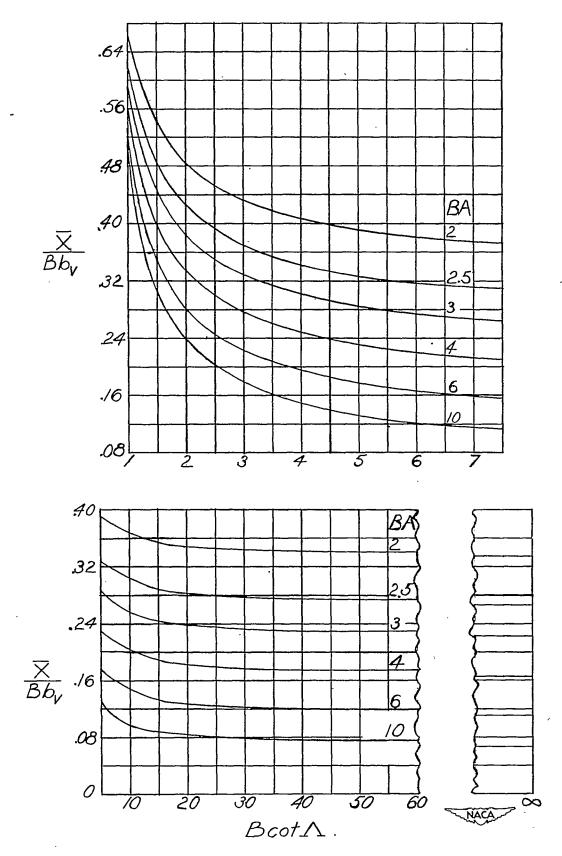
(c) Illustrative variation with sweep angle. A = 2; λ = 0.5; M = 2.

Figure 8.- Continued.
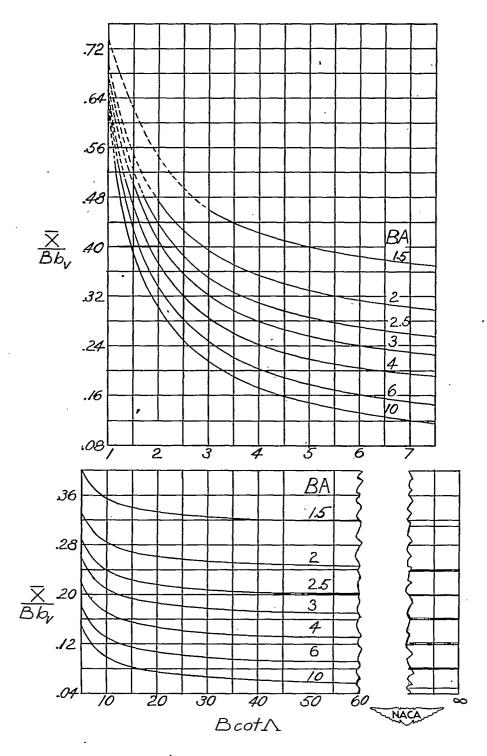
(d) Illustrative variation with taper ratio. $M = 2$; $A = 2$; $\Lambda = 53^{\circ}$.

Figure 8.- Concluded.

7
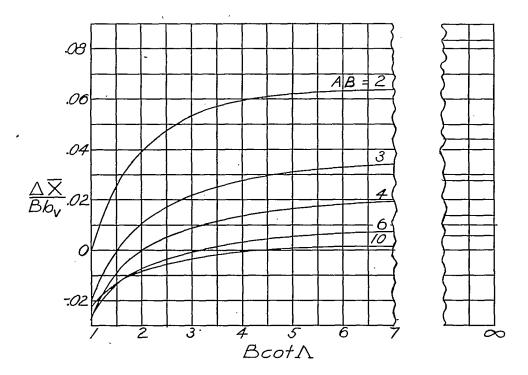
(a) Taper ratio of 0.

Figure 9.- Variation of $\overline{X}/Bb_v$ with $B \cot \Lambda$ for various values of BA and for taper ratios of 0 and 1.
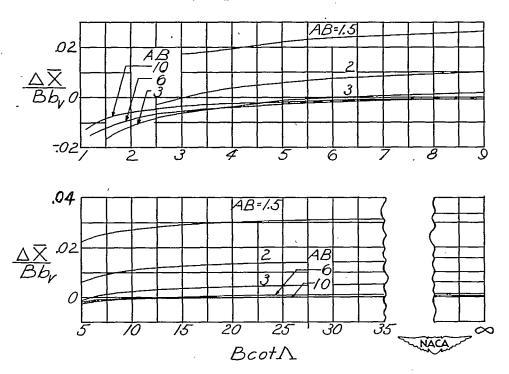
(b) Taper ratio of 1.

Figure 9.- Concluded.
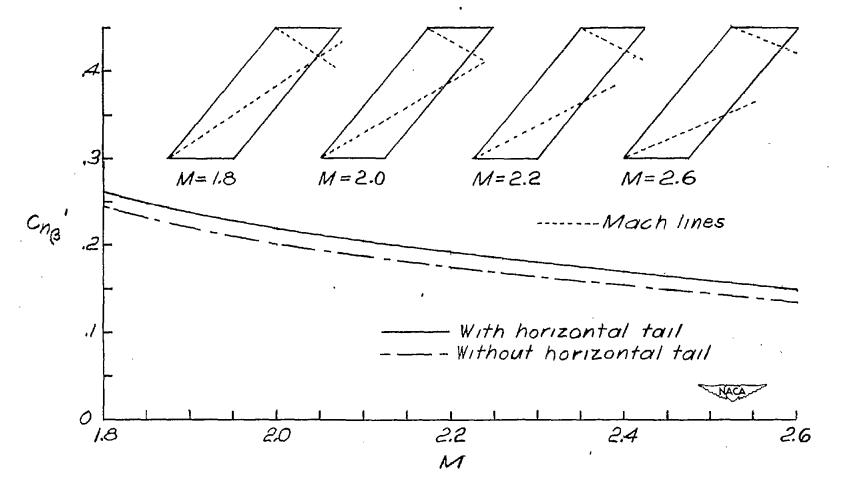
(a) Taper ratio of 0.
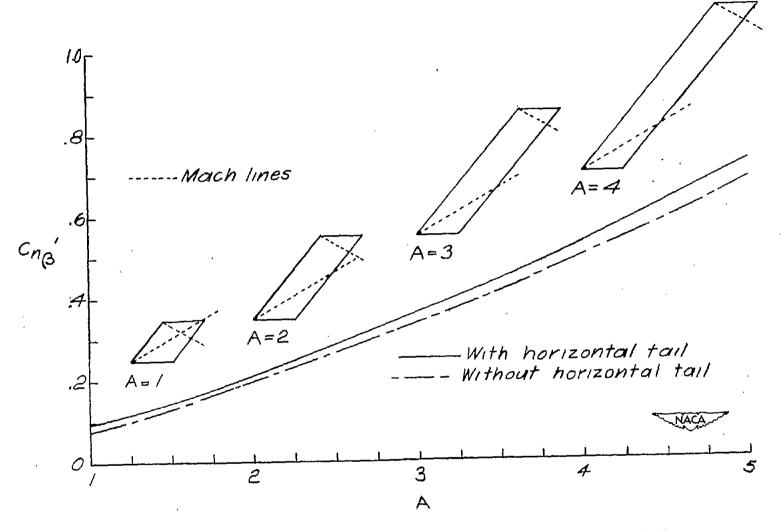
(b) Taper ratio of 1.

Figure 10.- Variation of $\Delta\overline{X}/Bb_V$ with $B \cot \Lambda$ for various values of BA and for taper ratios of 0 and 1.
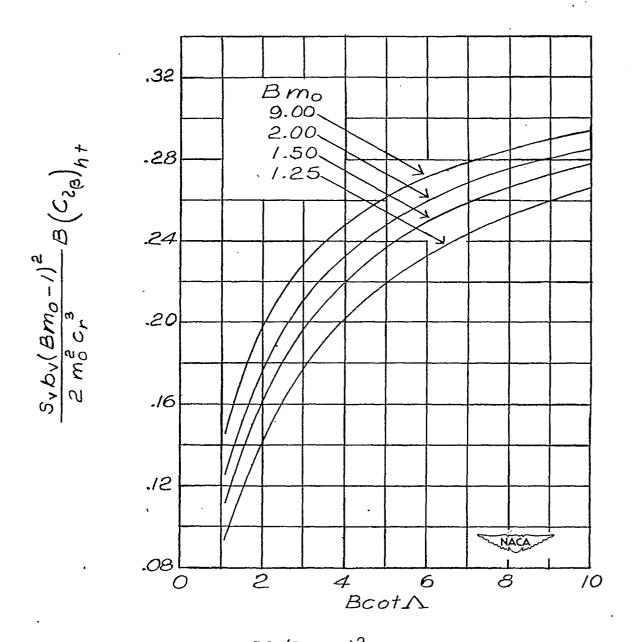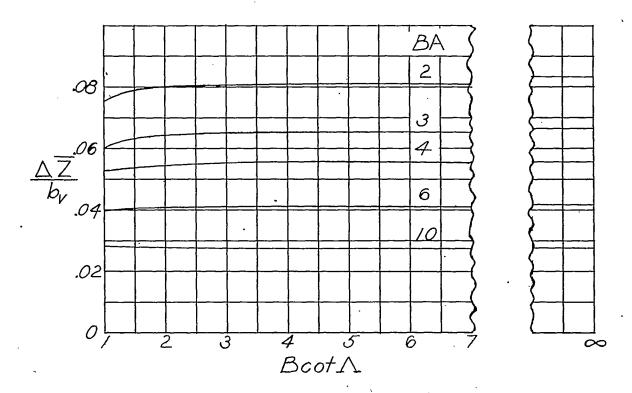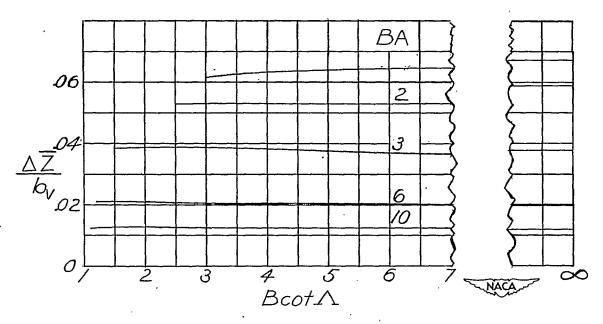
(a) Illustrative variation with Mach number. $A = 2$; $\lambda = 1.0$; $\Lambda = 40^\circ$.

Figure 11.- Some illustrative variations of $C_{n_\beta}{}'$ with Mach number, aspect ratio, and sweep angle for $\dfrac{S_W}{c_r{}^2} = 10$, $\dfrac{b_W}{c_r} = 8$, $\dfrac{l_t}{c_r} = 3$, and $\alpha = 0$.

(b) Illustrative variation with aspect ratio. M = 2; λ = 1; Λ = 40°.

Figure 11.- Continued.

(c) Illustrative variation with sweep angle. $\lambda = 1$; $M = 2$; $A = 2$.
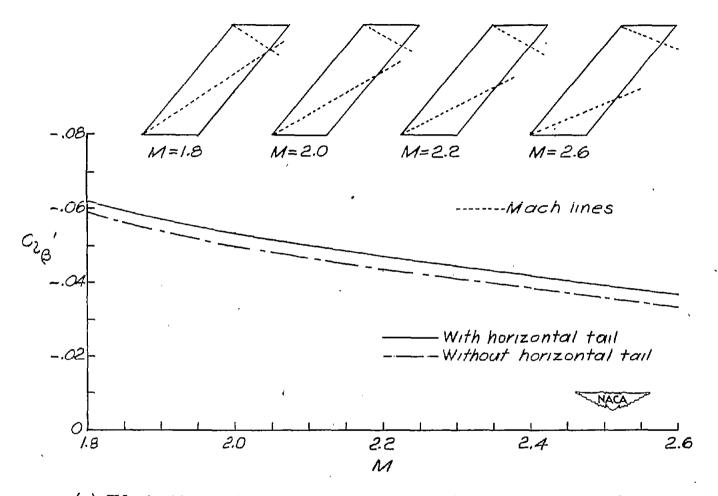
Figure 11.- Concluded.

(a) Taper ratio of 0.

(b) Taper ratio of 1.

Figure 12.- Variation of $\bar{Z}/b_V$ with B cot Λ for various values of BA
and for taper ratios of 0 and 1.

Figure 13.- Variation of $\dfrac{S_v b_v (Bm_0 - 1)^2}{2m_0{}^2 c_r{}^3} B\left(C_{l_\beta}\right)_{ht}$ with $B \cot \Lambda$ for various values of Bm_0.
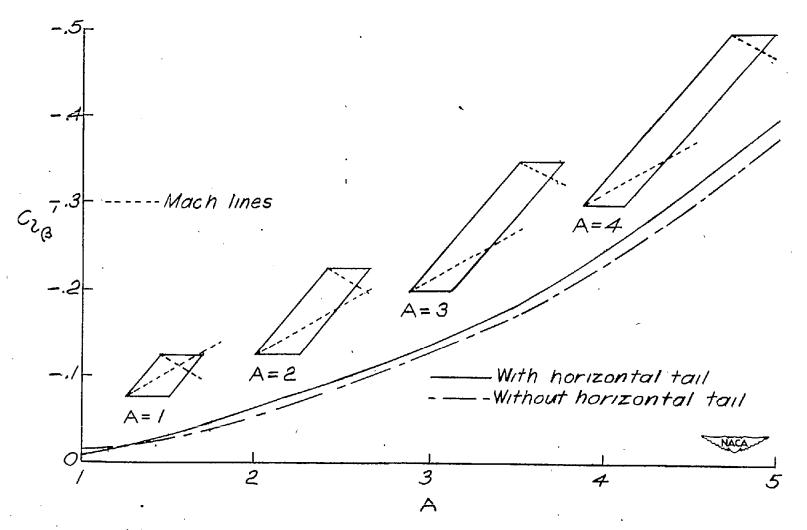
(a) Taper ratio of 0.

(b) Taper ratio of 1.

Figure 14.- Variation of $\Delta\overline{Z}/b_V$ with B cot Λ for various values of BA and taper ratios of 0 and 1.
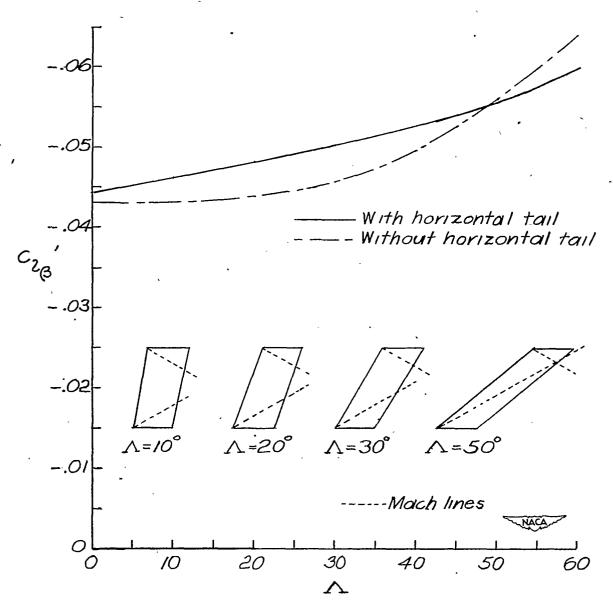
(a) Illustrative variation with Mach number. $A = 2$; $\lambda = 1.0$; $\Lambda = 40°$.

Figure 15.- Some illustrative variations of $C_{l_\beta}{}'$ with Mach number, aspect ratio, and sweep angle for $\dfrac{S_W}{c_r^2} = 10$, $\dfrac{b_V}{c_r} = 8$, and $\alpha = 0$.

(b) Illustrative variation with aspect ratio. M = 2; λ = 1; Λ = 40°.

Figure 15.- Continued.

(c) Illustrative variation with sweep angle. $\lambda = 1$; $M = 2$; $A = 2$.

Figure 15.- Concluded.